Electronic Supplementary Material (ESI) for ChemComm.

Supporting Information

Electrochemical removal of toxic metals from reaction media following catalysis

David R. Husbands,[a] Elisha M. Booth,[a] Niall W. B. Donaldson,[a] Nikil Kapur,[b] Rebecca M Willans,[a] Charlotte E. Willans*[a]

The authors wish to thank to Karl Heaton (mass spectrometry), Dr Richard Gammons and Dr Adrian Whitwood (X-ray crystallography), Dr Scott Hicks and Dr Chris Horbaczewskyj for their help with LC method development, and Prof. Ian Fairlamb for useful discussions.

Contents

1. General Instrumentation details

NMR spectra were obtained using a Bruker AVIIIHD 600 Widebore instrument 600 MHz [^{1}H], 565 MHz [^{19}F], 243 MHz [^{31}P], 151 MHz [^{13}C]). Chemical shifts (δ) are reported in parts per million (ppm) and were referenced to the residual non-deuterated solvent of the deuterated solvent used; $CDCl_3$: δ ^{1}H = 7.26 ($CHCl_3$) and ^{13}C = 77.16 ($CDCl_3$); DMSO-d_6 δ ^{1}H = 2.50 (CHD_2SOCD_3), ^{13}C = 39.52 (CD_3SOCD_3).[1] Spectral data were collected at 298 K (25 °C), unless stated otherwise. All ^{1}H NMR signals and integrals are reported as they appear in the spectrum.

^{31}P NMR spectral data were collected with proton decoupling, unless otherwise stated. Chemical shifts for ^{31}P resonances were calibrated by externally referencing to 85% H_3PO_4 in H_2O (w/w). This was practically carried out by inserting a sealed, vacuum-dried capillary tube containing 85% H_3PO_4 in H_2O (w/w) into an NMR tube containing the sample of interest, collecting a ^{31}P NMR spectrum and setting the H_3PO_4 resonance to 0 ppm. ^{19}F spectral data were referenced in the same manner using α,α,α-trifluorotoluene (-63.72 ppm with respect to $CFCl_3$). All ^{13}C NMR spectra were obtained with ^{1}H decoupling. All NMR spectra were processed using MestReNova (MNova) software (v. 14).

HRMS ESI-MS data were measured using a Bruker Daltronics micrOTOF MS, Agilent series 1200LC with electrospray ionization (ESI) or on a Thermo LCQ using electrospray ionization, with <5 ppm error recorded for all HRMS samples. HRMS GC-EI (electron impact) was collected using an Agilent 7890B gas chromatograph (start temp. = 60 °C, hold time = 1 min, ramp rate = 30 °C min^{-1}, end temp. = 300 °C, hold time = 6 min, total time = 15 min., injector temperature = 280 °C, He carrier gas flow rate = 1 mL min^{-1}) coupled to a JEOL AccuTOF GCx-plus MS. Mass to charge ratios (*m/z*) are reported in Daltons. ESI ions are reported as the $[M+H]^+$ cation, unless a Na or K is present in the molecular formula, in which case the $[M+Na]^+$ or $[M+K]^+$ ion is being measured.

Infrared (IR) spectra were obtained using a Bruker ALPHA-Platinum FTIR Spectrometer with a platinum-diamond ATR sampling module. Melting points were determined using a Stuart® SMP3 Melting Point machine. UV-Vis spectra and time course data were obtained using a Jasco V-560 UV-Vis Spectrophotometer fitted with a Julabo F12 thermostatically controlled water bath and circulator. UV-Vis cuvettes were Hellma Analytics® QG synthetic quartz glass (path length 10.00 mm).

Liquid Chromatography (LC) was performed using an UltiMate® 3000 series High-Performance Liquid Chromatography instrument, fitted with a Photodiode Array Detector. It was connected to a Bruker HCTultra ETD II equire^{TM} series ion trap mass spectrometer for aid in peak identification. LC data at 280 nm was processed using Bruker Compass DataAnalysis v. 4.4 (Build 102.47.2299).

Cyclic voltammograms were collected using an Metrohm Autolab potentiostat, and processed using Nova 2.1.6 software and OriginPro 2023b. Inductively Coupled Plasma (ICP) elemental analysis and quantification was carried out using an Agilent ICP-OES 5800 VDV spectrometer.

Diffraction data were collected at 110 K on an Oxford Diffraction SuperNova diffractometer with Cu-K_α radiation (λ = 1.54184 Å) or Mo-K_α radiation (λ = 0.71073), using an EOS CCD camera. The crystal was cooled with an Oxford Instruments Cryojet. Diffractometer control, data collection, initial unit cell determination, frame integration and unit-cell refinement was carried out with "Crysalis".[2] Face-indexed absorption corrections were applied using spherical harmonics, implemented in SCALE3 ABSPACK scaling algorithm.[3] OLEX2[4] was used for overall structure solution and refinement . Within OLEX2, the algorithm used for structure solution was "ShelXT dual-space".[5] Refinement was carried out by full-matrix least-squares used the SHELXL-97[5] algorithm within OLEX2. All non-hydrogen atoms were refined anisotropically. Crystalmaker® software was used to visualize the structures as well as generating the figures presented herein.

2. Synthesis

2.1. ^{t}Bu-Schiff Ligand 1

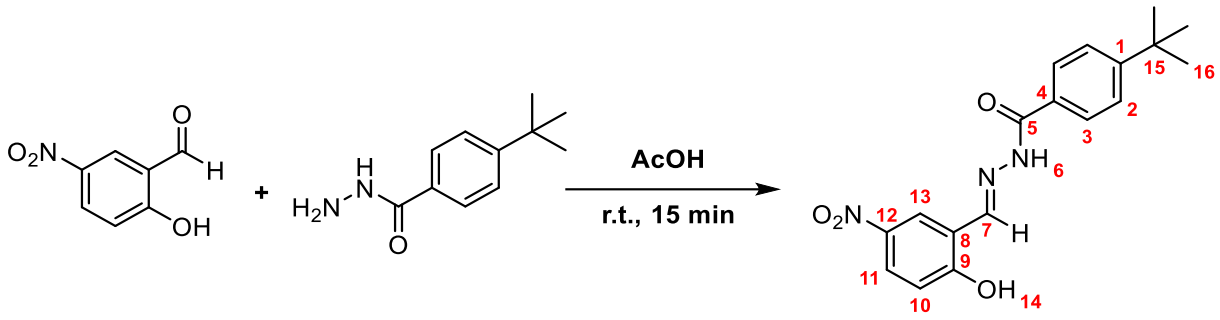

(*E*)-4-(*tert*-butyl)-*N*'-(2-hydroxy-5-nitrobenzylidene)benzohydrazide

Method adapted from Jacq *et al.*[6]

5-Nitrosalicylaldehyde (836 mg, 5.0 mmol, 1 equiv.) was dissolved in glacial acetic acid (20 mL) in a round bottomed flask, followed by 4-tert-butylbenzoic hydrazide (961 mg, 5.0 mmol, 1 equiv.). The reaction was stirred at room temperature for 15 minutes, during which time a beige precipitate formed. The reaction mixture was poured into cold water (60 mL), and the precipitate isolated by filtration, washed (water, then pentane) and dried under a flow of air to give the isolated product. The product was further dried overnight *in vacuo* to remove residual solvent, giving the pure product as a beige powder (1.51 g, 4.42 mmol, 88 %); ^{1}H NMR (600 MHz, DMSO-d_6) δ 12.36 (s, 1H, H-6), 12.21 (s, 1H, H-14), 8.73 (s, 1H, H-7), 8.58 (d, J = 2.9 Hz, 1H, H-13), 8.16 (dd, J = 9.0, 2.9 Hz, 1H, H-11), 7.89 (d, J = 8.1 Hz, 2H, H-3), 7.56 (d, J = 8.1 Hz, 2H, H-2), 7.11 (d, J = 9.0 Hz, 1H, H-10), 1.31 (s, 9H, H-16); ^{13}C NMR (151 MHz, DMSO-d_6) δ 163.0 (C-9), 162.6 (C-5), 155.1 (C-1), 144.2 (C-7), 139.9 (C-12), 129.9 (C-4), 127.6 (C-3), 126.5 (C-11), 125.3 (C-2), 123.9 (C-13), 120.0 (C-8), 117.1 (C-10), 34.7 (C-15), 30.9 (C-16); HRMS (ESI^{+}) $(C_{18}H_{19}N_3NaO_4)^{+}$ *m/z* (calculated) 364.1268, (found) 364.1272, mass difference 0.9 ppm; (ATIR): $\tilde{\nu}$ (cm^{-1}) 3564 (br, w, OH), 3353 (NH), 2957 (C-H aliphatic), 2905, 2869, 1674 (s, C=O amide), 1610, 1517, 1503, 1477, 1443, 1393, 1336, 1282 (vs), 1264, 1239, 1201, 1154, 1131, 1114, 1103, 940, 890, 861, 816, 783, 766, 743, 732, 722, 699, 637, 52, 472; m.p. 294.8 – 296.6 °C (acetic acid).

Single crystals suitable for XRD were obtained by recrystallisation from refluxing MeOH (approx. 200 mL for 200 mg of compound). Although this compound has been reported in the literature,[7] no accompanying characterisation data has been supplied.

Lab book ref. DRH-04-31

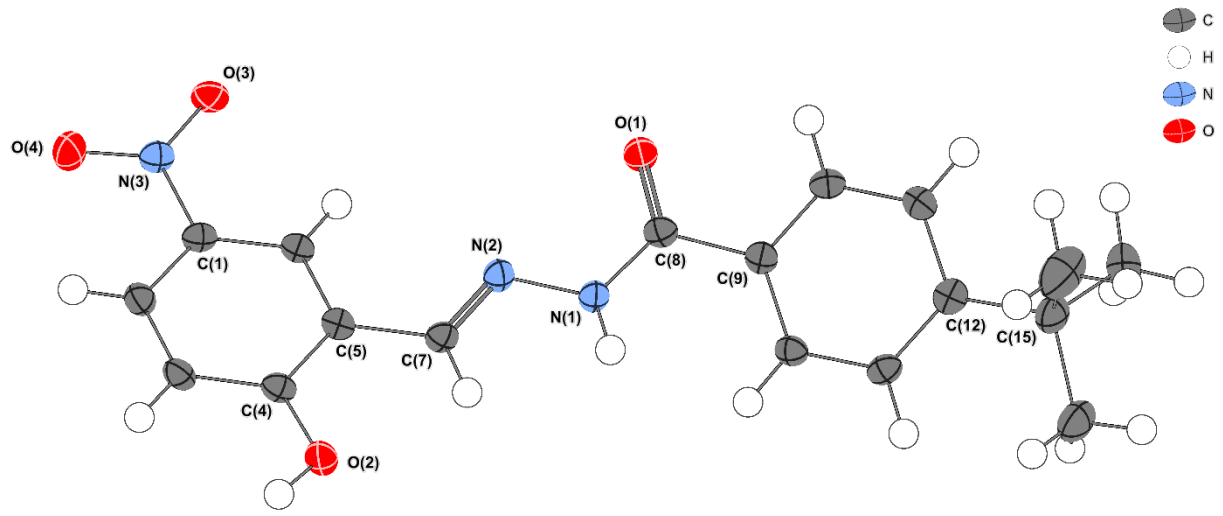

Figure S1: Structure, obtained by X-ray diffraction, of a single crystal of (E)-4-(tert-butyl)-N'-(2-hydroxy-5-nitrobenzylidene)benzohydrazide 1 (thermal ellipsoids are set at 50% probability). Selected interatomic lengths /Å: C1-N3 = 1.4525(17); C5-C7 = 1.4656(18); C7-N2 = 1.2779(18); N2-N1 = 1.3803(16); N1-C8 = 1.3518(18); C8-O1 = 1.2339(17). Selected interatomic angles /°: C5-C7-N2 = 120.94(12); C7-N2-N1 = 114.38(11); N2-N1-C8 = 119.83(11); C1-C5-C6 = 119.08(12); C9-C10-C11 = 120.66(13). The adopted conformation of this structure is due to H-bond stabilisation between molecules, primarily between O2-H2a-O3' = 1.74(3) Å, angle 168(2) °, and N1-H1-O3' = 2.194(18) Å, angle 160.2(13) °.

Table S1: X-Ray data for (E)-4-(tert-butyl)-N'-(2-hydroxy-5-nitrobenzylidene)benzohydrazide 1

Identification code	cew24001
Empirical formula	$C_{18}H_{19}N_3O_4$
Formula weight	341.36
Temperature/K	110.00(10)
Crystal system	monoclinic
Space group	$P2_1/c$
a/Å	11.6692(4)
b/Å	12.8126(5)
c/Å	11.3946(5)
α/°	90
β/°	97.665(3)
γ/°	90
Volume/Å^3	1688.41(11)
Z	4
ρ_{calc}g/cm^3	1.343
μ/mm^{-1}	0.797
F(000)	720.0
Crystal size/mm^3	0.293 × 0.258 × 0.135
Radiation	Cu Kα (λ = 1.54184)
2Θ range for data collection/°	7.644 to 134.16
Index ranges	-13 ≤ h ≤ 13, -15 ≤ k ≤ 14, -12 ≤ l ≤ 13

Reflections collected	9320
Independent reflections	3013 [R_{int} = 0.0270, R_{sigma} = 0.0333]
Data/restraints/parameters	3013/0/237
Goodness-of-fit on F^2	1.048
Final R indexes [I>=2σ (I)]	R_1 = 0.0371, wR_2 = 0.1024
Final R indexes [all data]	R_1 = 0.0418, wR_2 = 0.1061
Largest diff. peak/hole / e $Å^{-3}$	0.29/-0.20
Identification code	cew24001

2.2. Ligand-Ni complex 2

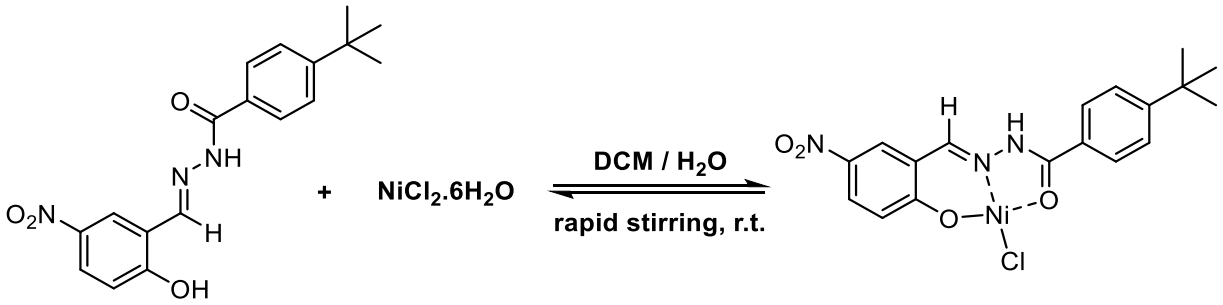

An attempt to synthesise and characterise the proposed Ni-ligand complex was undertaken. Ligand **1** (50 mg, 0.146 mmol, 1 equiv.) and $NiCl_2.6H_2O$ (348 mg, 1.46 mmol, 10 equiv.) were charged into a Schlenk flask under atmospheric conditions. DCM (15 mL) and deionised water (10 mL) were added, and the reaction stirred rapidly for 18 hours. It should be noted that the DCM layer contained a large quantity of insoluble orange material, which turned yellow-green after approximately 10 min. A small portion of the DCM layer was taken for analysis using UV-Vis spectroscopy (~50 µL in 2.5 mL of MeCN / H_2O (75:25 v/v)) and two new large peaks were observed at 398 and 286 nm, corresponding to the proposed Ni complex. After 18 hours, the water layer was decanted, and the DCM layer was washed with water (4 x 20 mL, by rapid stirring in the Schlenk tube followed by decanting), and the DCM layer was evaporated *in vacuo* to give a green-yellow solid (49 mg). Analysis of this solid proved challenging due to its extremely low solubility in all tested solvents. An NMR spectrum in DMSO-d_6 gave two new peaks at ^{1}H δ 9.71 and 9.41 ppm (compared to free ligand **1**), which could be the bound complex, but it is likely that the complex is in equilibrium in DMSO. FTIR showed new stretches in the OH/NH region (3000-3500 cm^{-1}), again suggesting a mixture of species is present. It was not possible to obtain mass spectrometric information on this complex due to extremely low solubility.

Lab book ref. DRH-04-40

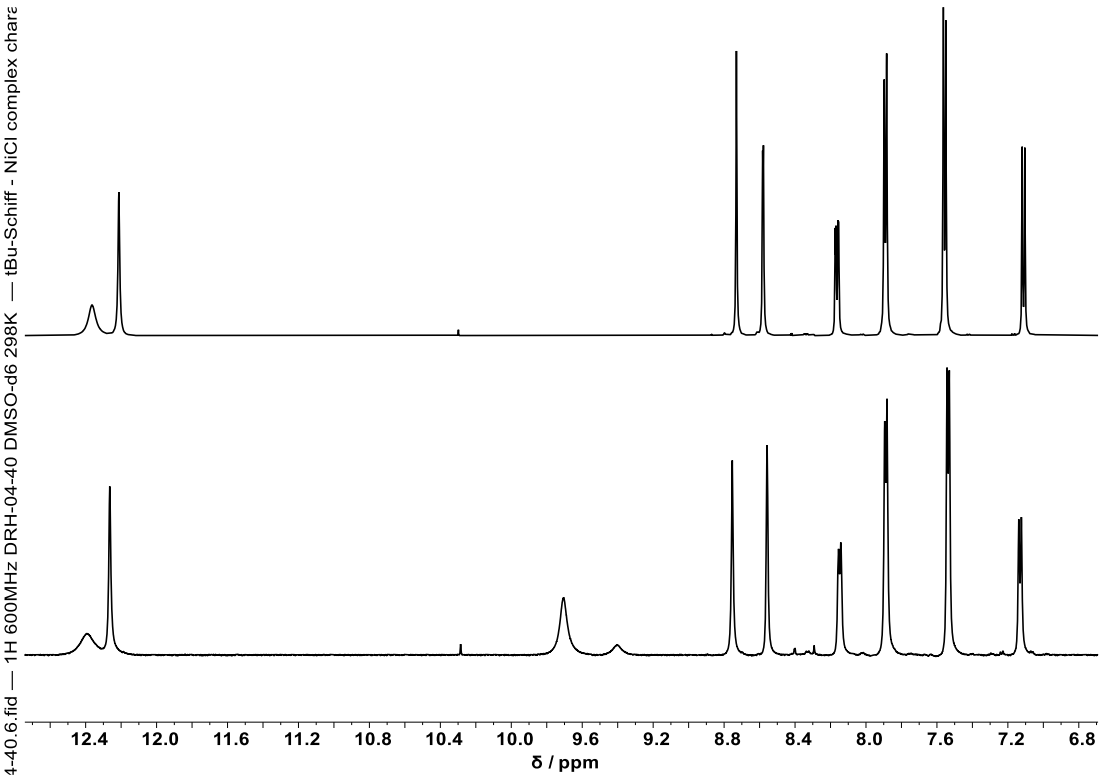

Figure S2: ^{1}H NMR spectra (600 MHz, DMSO-d_6, 298 K) of the aromatic region of ligand 1 (top) (lab book ref. DRH-04-35), and proposed complex 2 (bottom) (lab book ref. DRH-04-40).

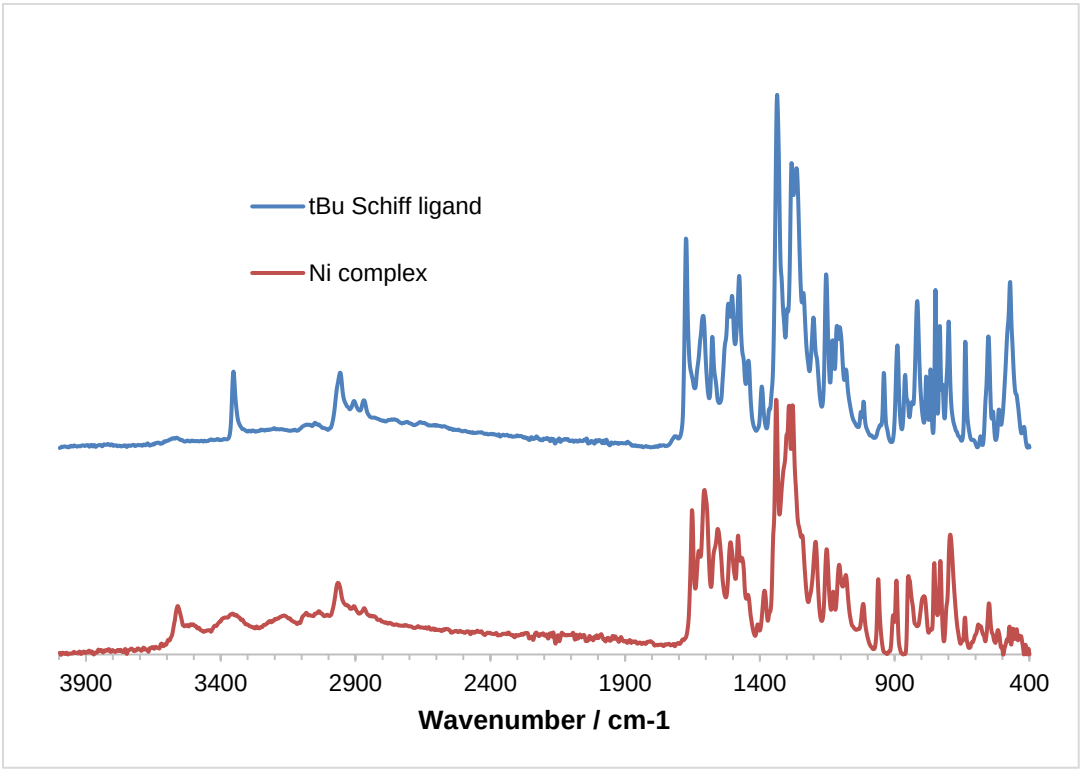

Figure S3: FTIR spectra of ligand 1 (top) (lab book ref. DRH-04-35), and proposed complex 2 (bottom) (lab book ref. DRH-04-40).

3. Eyring analysis of Ligand-Metal Binding

A stock solution of ^{t}Bu-Schiff ligand **1** in MeCN/H_2O (75:25 v/v) was prepared at 0.000318 mmol g^{-1} concentration. Separately, a stock solution of $NiCl_2.6H_2O$ in MeCN/H_2O (75:25 v/v) was prepared at 0.00920 mmol g^{-1} concentration. 2.50 mL (2.171 g) of ligand **1** stock solution was transferred to a quartz glass cuvette and sealed with a rubber septum. The cuvette and a separate reference solution of MeCN/H_2O (75:25 v/v) were placed in the UV-Vis spectrometer. The samples were heated by a water-jacket in the spectrometer, and the temperature of the samples were allowed to equilibrate for 15 minutes. The temperature of the reference sample was taken using an external thermocouple after this time. After an initial UV-Vis spectrum was taken, 100 µL of $NiCl_2$ stock solution (0.089 g, 15 equiv.) was rapidly injected into the cuvette via the rubber septum, the entire sample was shaken vigorously to ensure mixing and a UV-Vis time course was immediately begun, monitoring the absorbance at 390 nm. After the reaction had reached completion, a final UV-Vis spectrum was taken.

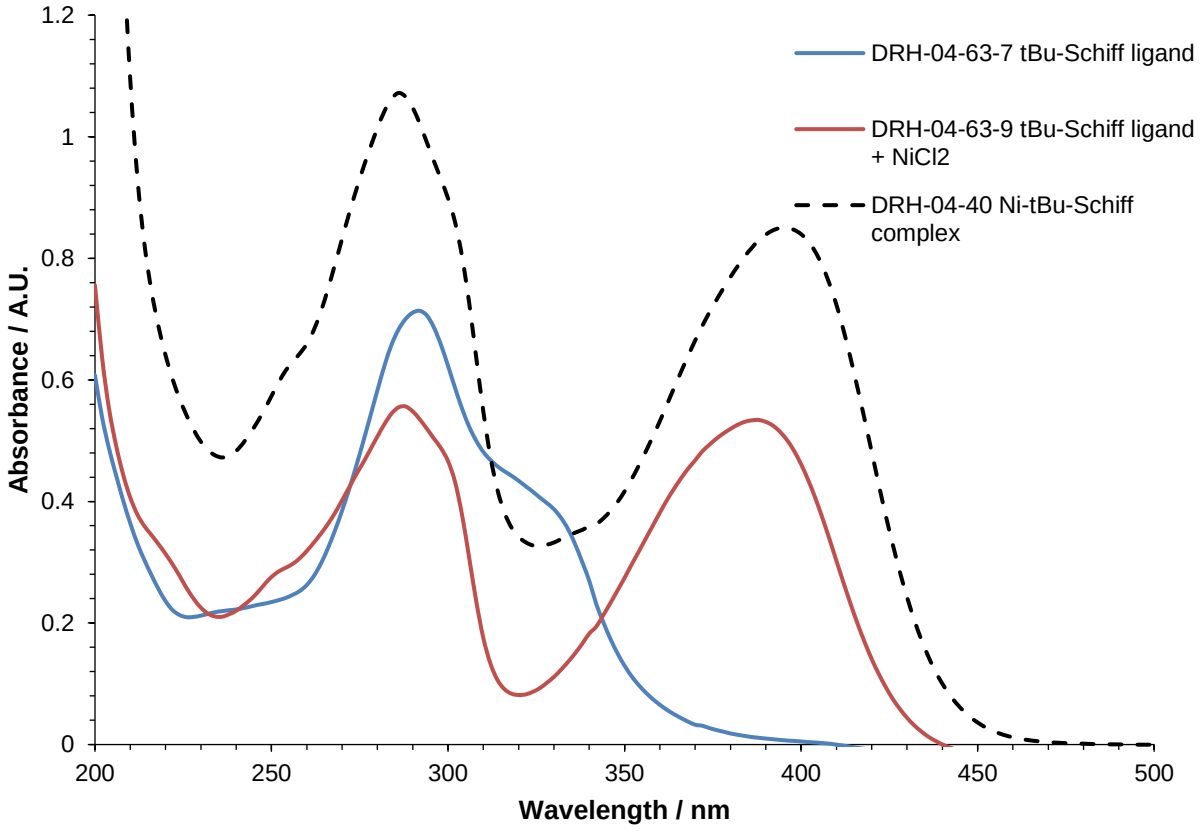

Figure S4: Compiled UV-Vis spectra showing free ligand 1 (blue), ligand 1 + $NiCl_2$ after a time course (red), and independently synthesised proposed complex 2 (dashed) (lab book ref. DRH-04-40).

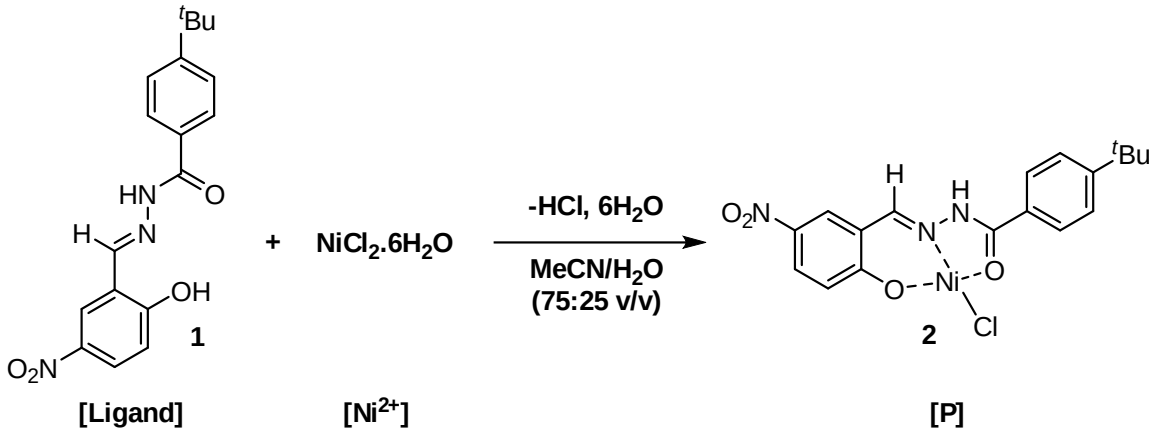

[Ligand] **[Ni^{2+}]** **[P]**

To determine the thermodynamic parameters of ligand binding *via* kinetic reaction rate experiments and Eyring analysis, a series of pseudo-first order reactions (using 15 equiv. of $NiCl_2.6H_2O$) were performed at different temperatures and product formation monitored by UV-Vis spectroscopy. Formation of the bound ligand-Ni complex was followed by observing a new absorbance band growing in at 390 nm over time. First-order fitting on the data was performed using OriginPro 2023b (ExpDec1 function, equation);

$$y = A_1 e^{\left(-\frac{x}{t_1}\right)} + y_0, \qquad where\ k_{obs} = \frac{1}{t_1}, \qquad and\ k = \frac{k_{obs}}{[Ni]}$$

Assuming that the concentration of $NiCl_2.6H_2O$ was constant, it was possible to determine the rate constant for the reaction at different temperatures. Using the Eyring equation;

$$ln\left(\frac{k}{T}\right) = \frac{-\Delta H^{\neq}}{R}\frac{1}{T} + ln\left(\frac{k_B}{h}\right) + \frac{\Delta S^{\neq}}{R}$$

a plot of ln(k/T) vs. 1/T (where k is the rate constant and T is the reaction temperature), it is possible to determine the thermodynamic parameters of ligand-metal binding for this process.

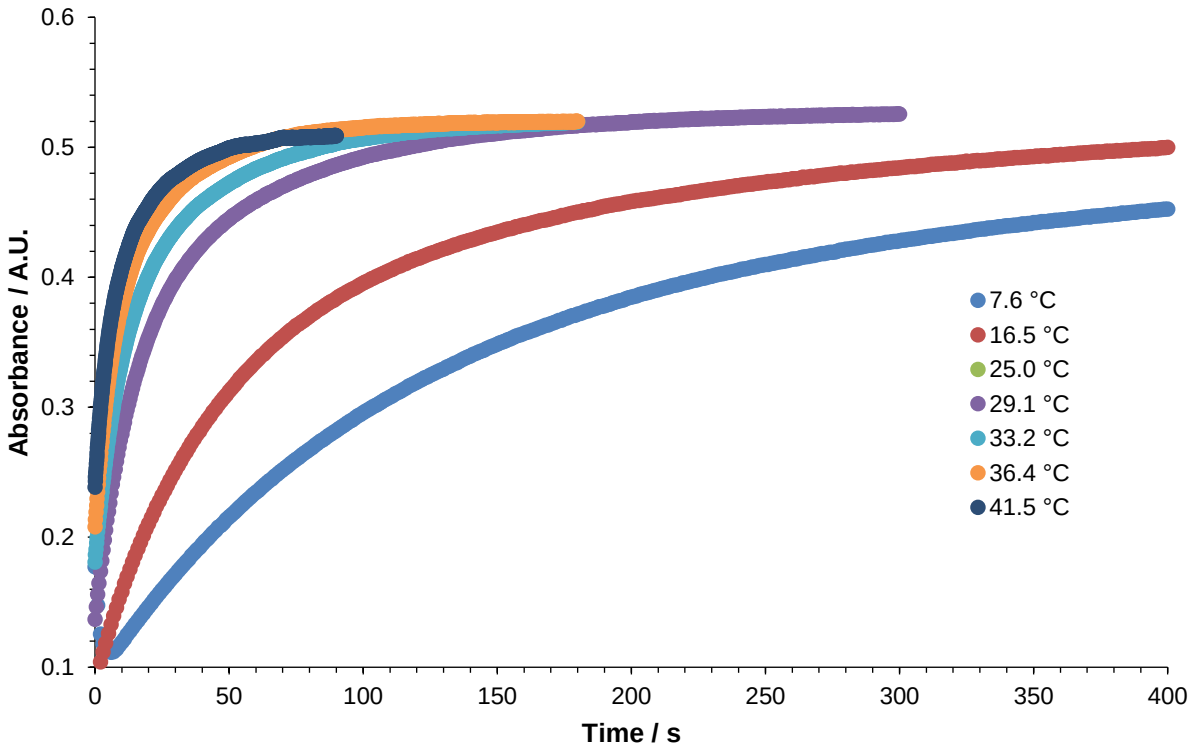

Figure S5: Absorbance *vs* time plots for the ligand binding at different concentrations. The wavelength monitored was 390 nm.

As the absorbance is low (less than 1 A.U.), it is assumed that absorbance ∝ concentration. As such, using rate = k_{obs}[ligand] with 1st order fitting, it is possible to obtain the rate constants for this reaction.

Table S2: The fitted rate constants at different temperatures for binding of ligand 1 with $NiCl_2.6H_2O$.

Data collection time: data pitch	Water bath temperature / °C	Sample temperature / K	k_{obs} / s^{-1}	k/ s^{-1}
1200 s : 1 s	5	280.75	0.005457	15.09128
1200 s : 1 s	15	289.65	0.009648	26.6809
600 s : 0.5 s	25	298.15	0.019696	54.46869
300 s : 0.5 s	30	302.25	0.030884	85.40979
180 s : 0.2 s	35	306.35	0.044256	122.3902
180 s : 0.2 s	40	309.55	0.058373	161.4306
90 s : 0.1 s	45	314.65	0.08164	225.7752

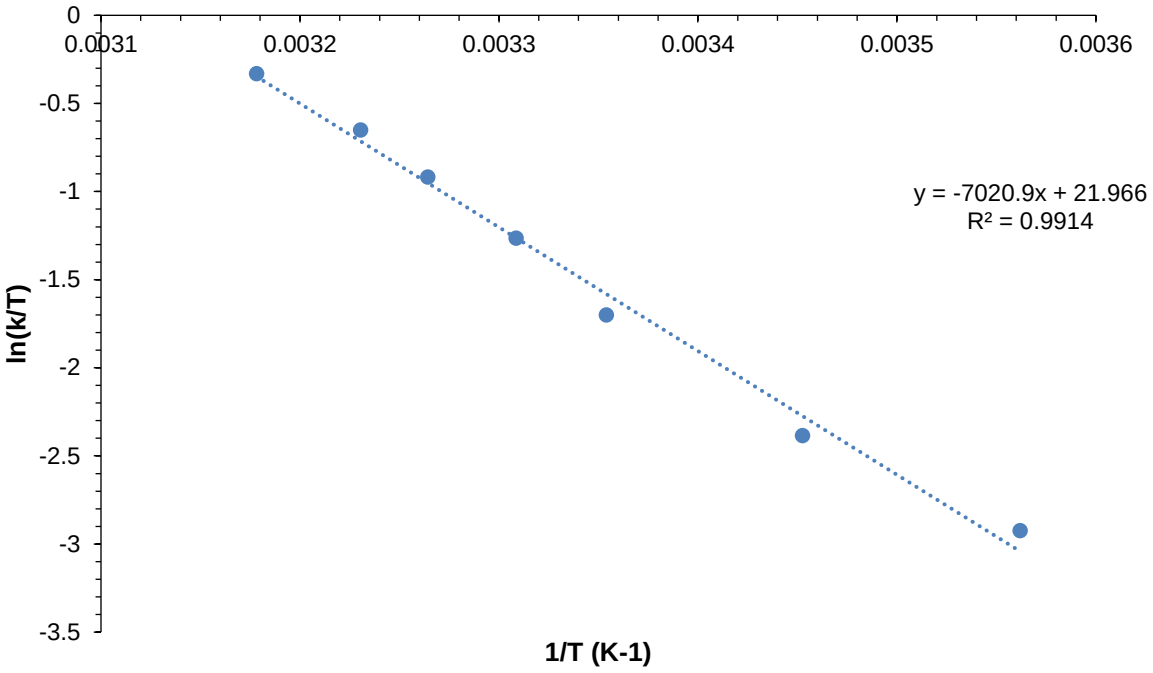

Figure S6: Eyring plot for binding of ligand 1 with $NiCl_2.6H_2O$.

Calculated Parameters (errors are calculated from linear regression of the fitted line)

$\Delta H^{\ddagger}$ = 58.4 ± 2.4 kJ mol^{-1}

$\Delta S^{\ddagger}$ = -14.9 ± 0.7 J K^{-1} mol^{-1}

$\Delta G^{\ddagger}$ = 62.8 ± 2.5 kJ mol^{-1}

(15.0 ± 0.6 kcal mol^{-1})

Lab book ref. DRH-04-63

4. Ni catalysed Suzuki-Miyaura cross-coupling reactions (SMCC)

4.1. NiCl(o-tolyl)(PPh_3)$_2$ (5) catalysed SMCC

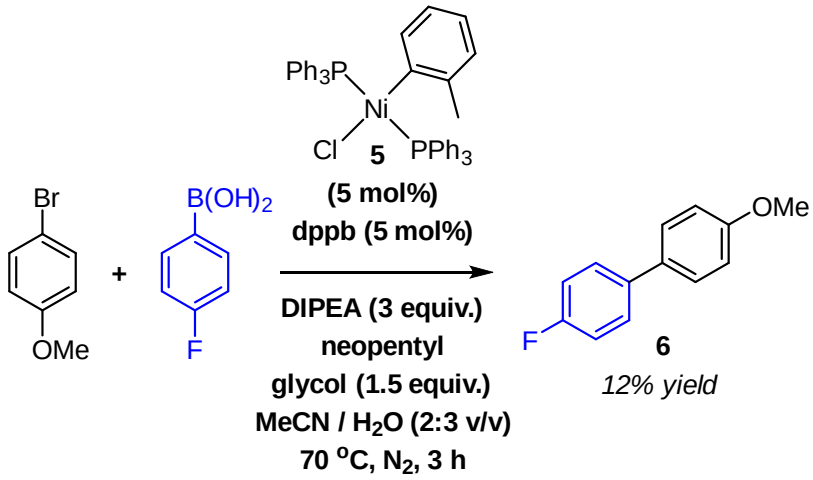

This reaction was modified from the literature.[8]

A 7 mL reaction vial was charged with 4-bromoanisole (63 µL, 0.5 mmol, 1 equiv.), 4-fluorophenylboronic acid (84.0 mg, 0.6 mmol, 1.2 equiv.), neopentyl glycol (78.1 mg, 0.75 mmol, 1.5 equiv.) and internal standard 1-fluoro-3,5-dimethyl-benzene (19.5 mg, 0.125 mmol, 0.25 equiv.) under argon. A fresh catalyst stock solution was prepared by adding NiCl(*o*-tolyl)(PPh_3)$_2$ pre-catalyst (35.5 mg, 10 mol%) and 1,4-bis(diphenylphosphino)butane (dppb) ligand precursor (21.3 mg, 10 mol%) to an argon-flushed ampoule. The solids were dissolved in anhydrous, degassed MeCN (2.4 mL) with the aid of sonication. 1.2 mL of the stock solution was transferred to the reaction vial *via* syringe (giving 5 mol% of catalyst and ligand), followed by degassed water (1.8 mL), producing a solvent system with a 2:3 (v/v) organic:aqueous solvent ratio. N,N-diisopropylethylamine (DIPEA) (261 µL, 1.5 mmol, 3 equiv.) was added and the vial was heated to 70 ºC with stirring, commencing the reaction. A 12% yield of cross-coupled product **6** (by HPLC) was observed after 2 hours which plateaued and remained as 12 % after 24 hours.

Lab book ref. EB012

4.2. $NiCl_2$(dppp) (4) catalysed SMCC

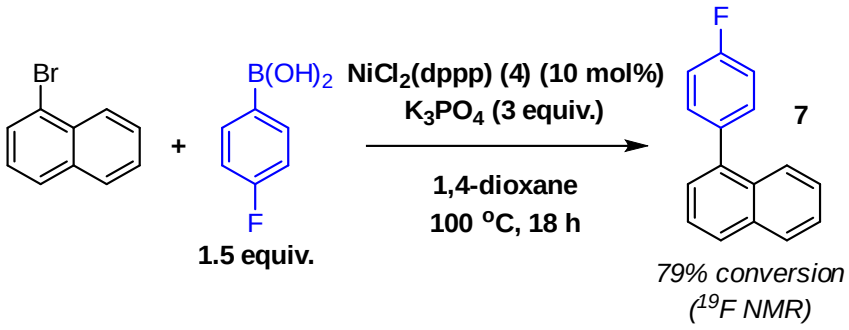

This reaction was modified from the literature.[9]

An ampoule was charged with $NiCl_2$(dppp) (269 mg, 0.5 mmol, 10 mol%), anhydrous K_3PO_4 (3172 mg, 15 mmol, 3 equiv.) and 4-fluorophenylboronic acid (1041 mg, 7.5 mmol, 1.5 equiv.). The vessel was evacuated and backfilled with nitrogen three times and kept under an atmosphere of nitrogen. Through a rubber septum, 1-bromonapthalene (0.7 mL, 1058 mg, 5 mmol, 1 equiv.) and anhydrous, degassed 1,4-dioxane (20 mL) were added, and the vessel was sealed under an atmosphere of nitrogen. The mixture was heated and vigorously stirred at 100 °C for 18 hours, before being allowed to cool and settle. 0.1 mL of the supernatant was taken and diluted with C*D*Cl_3 for NMR analysis. ^{19}F NMR gave a % conversion of 79% to product **7** (based on 1.5 equiv. of arylboronic acid).

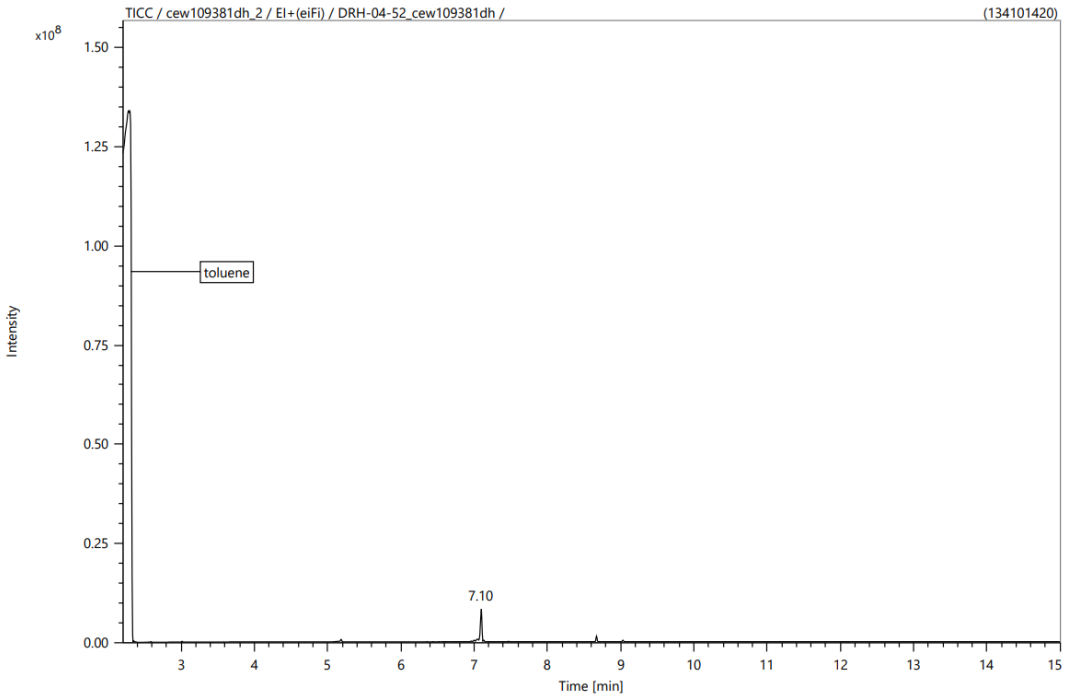

Figure S7: GC trace of the reaction mixture following catalysis.

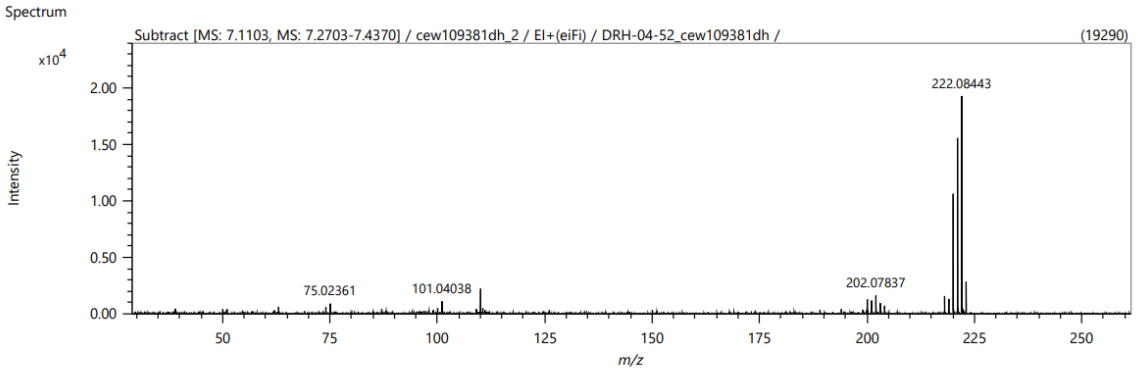

Elemental Composition

Parameters		Elements Set 2:			
Tolerance:	±10.00 ppm	Symbol	C	H	F
Electron:	Odd/Even	Min	4	4	0
Charge:	+1	Max	16	32	1
DBE:	-0.5 - 100.0				

Results

Mass	Intensity	Formula	Calculated Mass	Mass Difference [ppm]	DBE
222.08443	19289.89	C16 H11 F	222.08393	2.24	11.0

Figure S8: HRMS (EI) spectrum of the GC peak at retention time 7.10 min confirming the presence of the SMCC product 7.

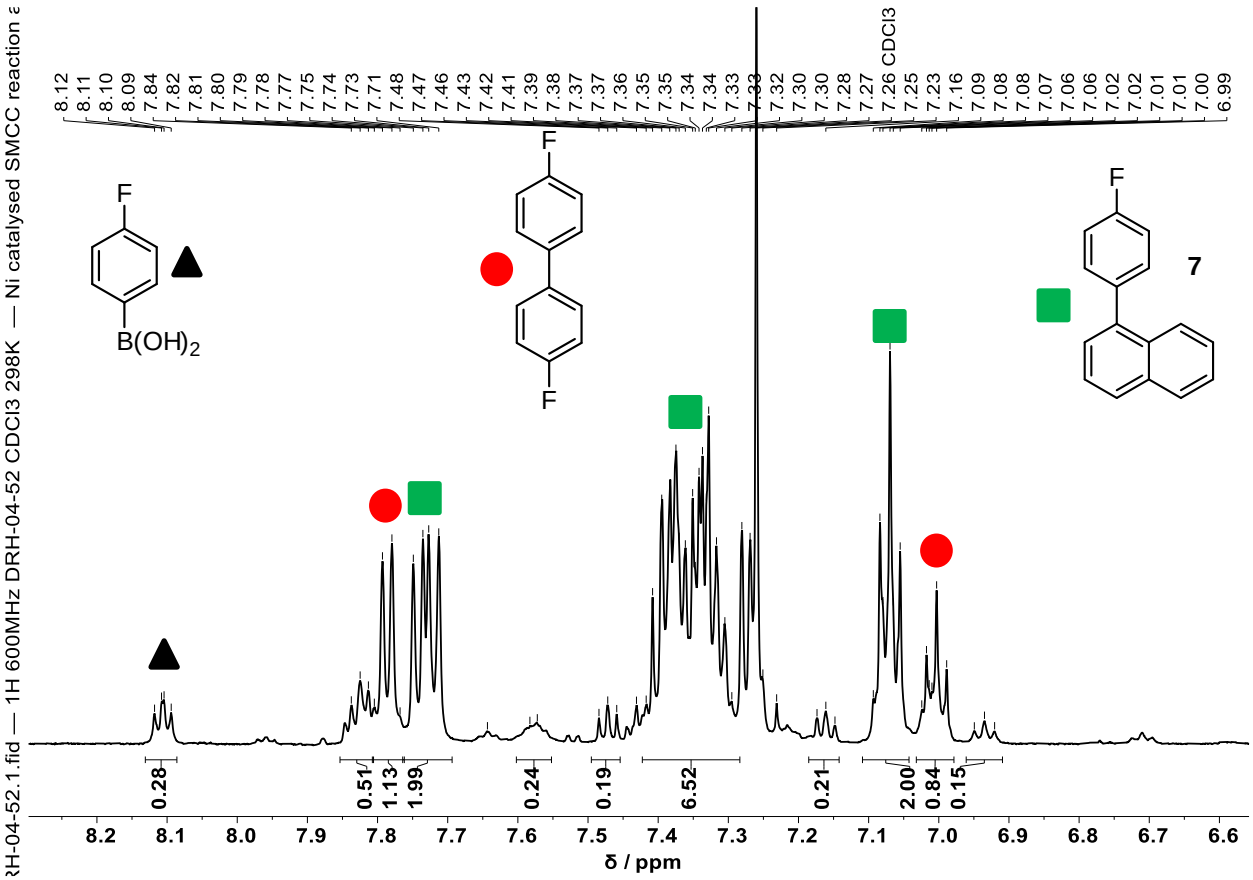

Figure S9: ^{1}H NMR (600 MHz, C*D*Cl$_3$, 298K) direct aliquot of the SMCC reaction mixture. The magnified aromatic region is displayed (omitting residual 1,4-dioxane solvent peaks). Key peaks of the product 7 (green squares), homo-coupled side-product (red circle) and residual arylboronic acid (black triangles) have been identified with reference to the ^{19}F NMR spectrum.

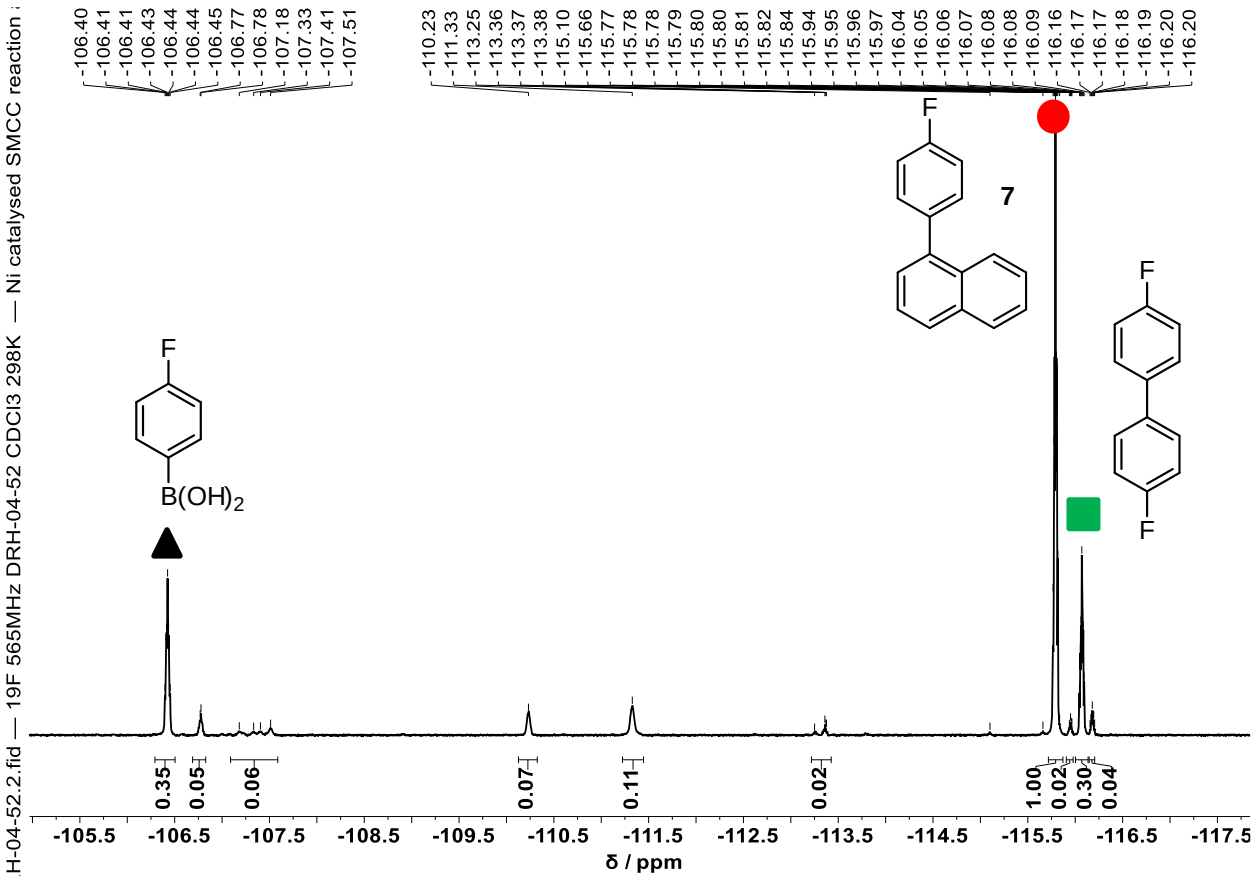

Figure S10: ^{19}F NMR (565 MHz, C*D*Cl$_3$, 298K) direct aliquot of the SMCC reaction mixture. Key peaks of the product 7 (green squares), homo-coupled side-product (red circle) and residual arylboronic acid (black triangles) have been identified with reference to the literature.[10,11] The % conversion to product was calculated using the integrals from this spectrum, accounting for the fact that 1.5 equiv. of arylboronic acid was used.

Lab book ref. DRH-04-52

5. Testing and development of LC method

5.1. Instrumentation

Liquid Chromatography (LC) was carried out using a Supelco® Ascentis® Express 90 Å C18 HPLC column (5 cm x 4.6 mm, 2.7 µm) fitted with a Supelco® Ascentis® Express 90 Å C18 Guard Column (0.5 cm x 4.6 mm, 2.7 µm). The solvent combination used was H_2O (0.1 % formic acid) and acetonitrile (0.1% formic acid), with a constant flow rate of 1.000 mL min^{-1}. The column was equilibrated for 30 min before each run with 50 % acetonitrile, and after each run was flushed with 10 % acetonitrile, then 100 % acetonitrile, then 50 % acetonitrile for 20 minutes each to remove any residues from the column.

The following method was used in all LC runs;

Table S3: LC method summary

Time / min	% acetonitrile	Flow rate / mL min^{-1}
0.00	50	1.000
5.00	100	1.000
6.00	100	1.000
6.20	50	1.000
8.00	50	1.000
10.00 (end of run)	50	1.000

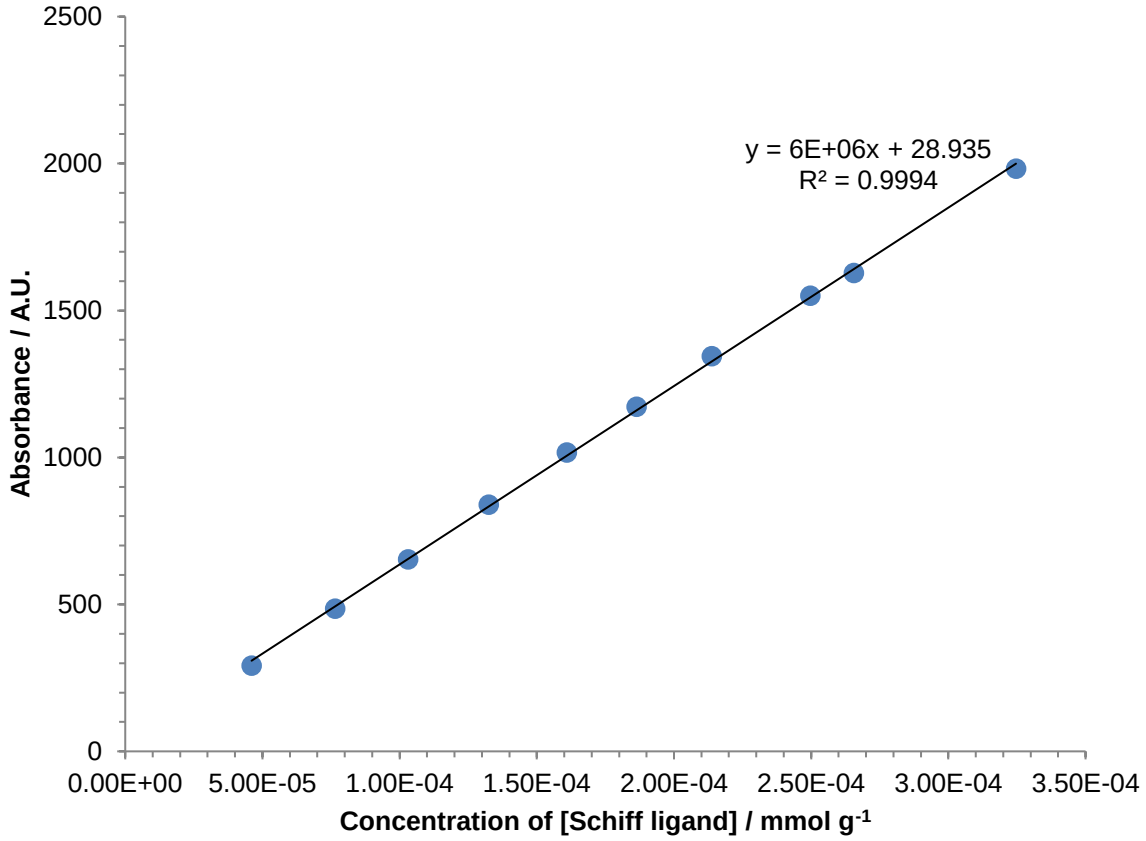

Figure S11: Calibration curve of ligand 1 in MeCN/H_2O (75:25 v/v). LCMS data lab book ref. DRH-04-38-1 to 10.

To determine that ligand **1** and Ni^{2+} bind in a 1:1 stoichiometry, LC experiments were run by increasing the concentration of NiCl(o-tolyl)(PPh_3)$_2$ compared to ligand **1** (up to ~1:1 stoichiometry). Figure S10 demonstrates that up to approximately 1:0.75 ligand:Ni ratio, the binding stoichiometry is linear, so this method is valid for determining [Ni] by consumption of ligand as excess ligand compared to Ni will be present. For ease of data processing, these calibrations were performed using the concentration unit mmol g^{-1} (mmol of **1** per g of solvent), allowing for rapid and accurate calibrations based upon mass of stock solutions rather than volumes. For subsequent calculations, mmol g^{-1} is converted back to conventional units of mM.

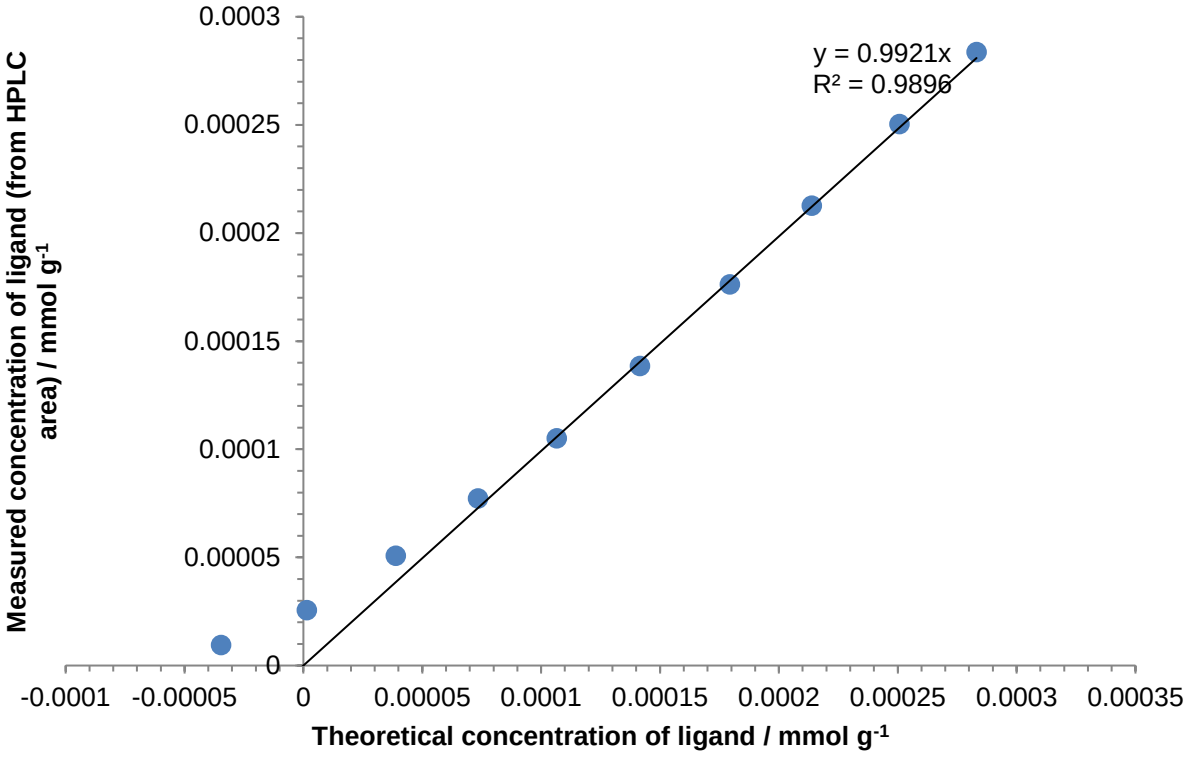

Figure S12: Stoichiometry binding test. The theoretical concentration of the ligand ($[ligand]_{max}$ – [Ni]) is plotted against the concentration of the ligand from LC data at different concentrations of [Ni]. LCMS data lab book ref. DRH-04-38-11 to 20.

5.2. Methodology

A stock solution of ligand **1** in MeCN/H_2O (75:25 v/v) was prepared (typically ~2.5 mM concentration). A known mass of ligand stock solution (of known concentration) was added to an HPLC vial, followed by a known mass of Ni-containing stock solution. This sample preparation was repeated at different masses of Ni-containing stock solution (effectively varying [Ni] in the sample), and the samples were analysed using the previously described LC method.

The peak area of ligand **1** (at retention time 2.6 min) was recorded, and using a spreadsheet the [Ni] in each sample was determined. This was done be comparing the observed concentration of ligand **1** to a pure LC sample of the ligand stock solution, with the difference between the two giving the concentration of [Ni] in the sample.

To improve accuracy in the measurements, a range of [Ni] were determined, and a plot of [Ni] vs. mass of Ni stock solution was produced to identify any anomalies. The ratio of [Ni]/[ligand] was calculated for each sample, and the determined [Ni] for each sample in the ratio range 0.1 – 0.6 was averaged to produce the final [Ni]. The reason for this is at high or very low [Ni], ligand binding is sigmoidal, so can lead to inaccurate results.

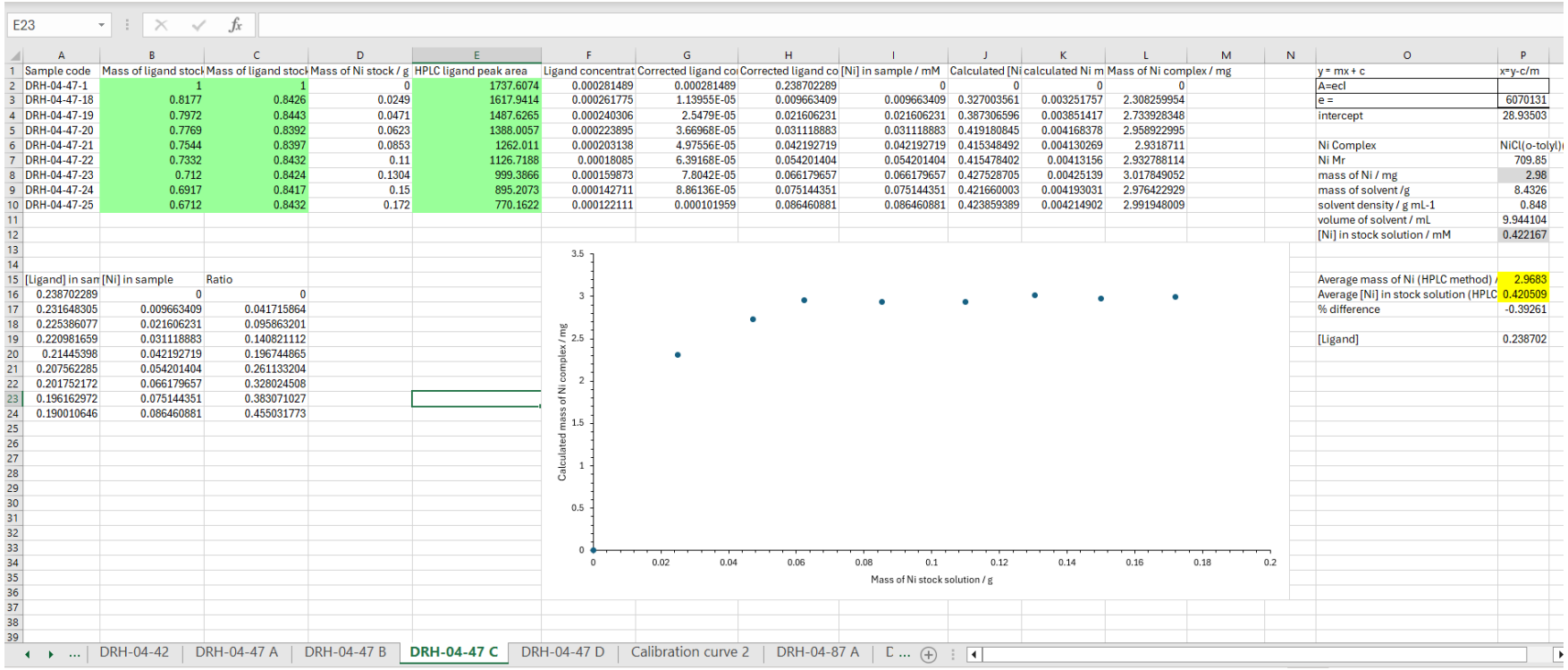

Sample code	Mass of ligand stock	Mass of ligand stock	Mass of Ni stock / g	HPLC ligand peak area	Ligand concentrat	Corrected ligand co	Corrected ligand co	[Ni] in sample / mM	Calculated [Ni	calculated Ni m	Mass of Ni complex / mg
DRH-04-47-1	1	1	0	1737.6074	0.000281489	0.000281489	0.238702289	0	0	0	0
DRH-04-47-18	0.8177	0.8426	0.0249	1617.9414	0.000261775	1.13955E-05	0.009663409	0.009663409	0.327003561	0.003251757	2.308259954
DRH-04-47-19	0.7972	0.8443	0.0471	1487.6265	0.000240306	2.5479E-05	0.021606231	0.021606231	0.387306596	0.003851417	2.733928348
DRH-04-47-20	0.7769	0.8392	0.0623	1388.0057	0.000223895	3.66968E-05	0.031118883	0.031118883	0.419180845	0.004168378	2.958922995
DRH-04-47-21	0.7544	0.8397	0.0853	1262.011	0.000203138	4.97556E-05	0.042192719	0.042192719	0.415348492	0.004130269	2.9318711
DRH-04-47-22	0.7332	0.8432	0.11	1126.7188	0.00018085	6.39168E-05	0.054201404	0.054201404	0.415478402	0.00413156	2.932788114
DRH-04-47-23	0.712	0.8424	0.1304	999.3866	0.000159873	7.8042E-05	0.066179657	0.066179657	0.427528705	0.00425139	3.017849052
DRH-04-47-24	0.6917	0.8417	0.15	895.2073	0.000142711	8.86136E-05	0.075144351	0.075144351	0.421660003	0.004193031	2.976422929
DRH-04-47-25	0.6712	0.8432	0.172	770.1622	0.000122111	0.000101959	0.086460881	0.086460881	0.423859389	0.004214902	2.991948009

[Ligand] in sam	[Ni] in sample	Ratio
0.238702289	0	0
0.231648305	0.009663409	0.041715864
0.225386077	0.021606231	0.095863201
0.220981659	0.031118883	0.140821112
0.21445398	0.042192719	0.196744865
0.207562285	0.054201404	0.261133204
0.201752172	0.066179657	0.328024508
0.196162972	0.075144351	0.383071027
0.190010646	0.086460881	0.455031773

y = mx + c	x=y-c/m
A=ecl	
e =	6070131
intercept	28.93503
Ni Complex	NiCl(o-tolyl)(
Ni Mr	709.85
mass of Ni / mg	2.98
mass of solvent /g	8.4326
solvent density / g mL-1	0.848
volume of solvent / mL	9.944104
[Ni] in stock solution / mM	0.422167
Average mass of Ni (HPLC method) /	2.9683
Average [Ni] in stock solution (HPLC	0.420509
% difference	-0.39261
[Ligand]	0.238702

DRH-04-42 | DRH-04-47 A | DRH-04-47 B | **DRH-04-47 C** | DRH-04-47 D | Calibration curve 2 | DRH-04-87 A

Figure S13: Example spreadsheet for DRH-04-47 C showing the calculation of [Ni] in the sample.

To use the accompanying spreadsheet (example shown in Figure XX), columns B (mass of ligand stock solution), C (mass of ligand stock solution and Ni stock solution) and E (area of the free ligand determined by LC) must be populated. The mass of Ni stock solution (column D) will be automatically calculated. A sample of the pure ligand stock solution must be run as a baseline point for $[ligand]_{max}$ (here DRH-04-47-1).

Using the calibration curve parameters, the ligand peak area is converted into absolute concentration (column F, example formula for DRH-04-47-19 cell F4 =(E4-O4)/O3), so must be corrected to account for the additional volume of Ni stock solution, and compared to the concentration of $[ligand]_{max}$. This is done in column G (example formula for DRH-04-47-19 cell G4 =((F2*B4)/C4)-F4. This is effectively the formula [Ni] = $[ligand]_{max}$ – $[ligand]_{measured}$.), which is the same value as the [Ni] in the sample (column H, [ligand] converted from mmol g^{-1} to mM). By using the masses of ligand stock and Ni stock in the LC sample, it is possible to calculate the [Ni] in the original stock solution (column J; example formula for cell J4 = (I4*C4)/D4). As the mass of solvent in the overall Ni stock solution (cell P9) and M_r of the Ni complex (cell P7) are known, the mmol of Ni (column K) and hence mass of Ni complex in the original stock solution (column L) can be calculated.

To improve the accuracy of the method, a range of [Ni] should be tested. A simple plot of calculated mass of Ni complex against the mass of Ni stock solution (Figure) shows that there should ideally be a linear binding region, which can be averaged to obtain the mass or concentration of Ni complex in solution. However, this can be misleading, and a better way to determine which data points should be integrated is by calculating the [Ni]/[ligand] ratio, shown in cells C15-24. Data points with the ratio 0.1 – 0.6 (ideally 0.5) should be averaged (barring anomolies). It should be noted that at too high or low [Ni] values, binding behaviour is not linear and can lead to unreliable results. As such, several concentrations should be tested to make sure that the linear binding regime is being calculated.

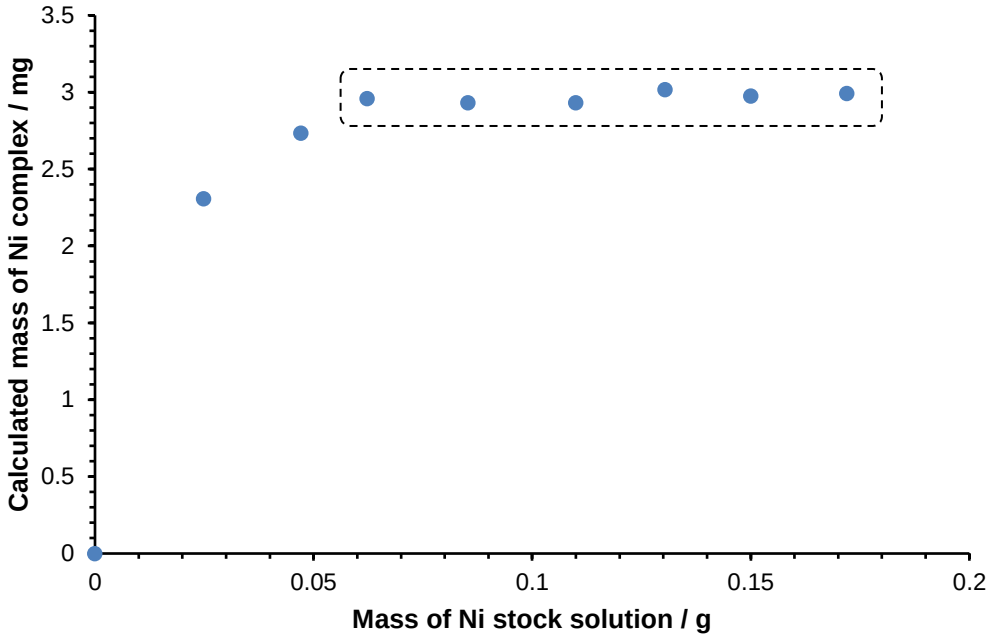

Figure S14: A plot of calculated mass of Ni complex against the mass of Ni stock solution for DRH-04-47 C. To calculate the average mass of Ni complex, an average of the "linear region" (denoted by the dotted box) of the graph is taken.

Table S4: Summary of calculated masses of Ni complexes using the LC method.

Code	Ni complex	Known [Ni] / mM	Calculated [Ni] (LC method) / mM	% Difference	([Ligand 1] / mM) [Ligand]/[Ni] ratio range
DRH-04-42[a] (1 – 10)	NiCl(o-tolyl)(PPh_3)$_2$	0.340	0.393	+ 15.5%	(0.270) 0.18 – 0.59
DRH-04-47 A[a] 2-9	NiCl(o-tolyl)(PPh_3)$_2$	0.605	0.618	+ 2.1%	(0.239) 0.15 – 0.55
DRH-04-47 B[a] (10-17	NiCl(o-tolyl)(PPh_3)$_2$	0.156	0.178	+ 14.5%	(0.239) 0.11 – 0.19

DRH-04-47 C[a] (18-25)	NiCl(o-tolyl)(PPh_3)$_2$	0.422	0.421	- 0.4%	(0.239) 0.14 – 0.46
DRH-04-47 D (26-33)	$NiBr_2(PPh_3)_2$	0.348	0.343	- 1.5%	(0.239) 0.12 – 0.37
DRH-04-87 A (2-6)[b]	$NiCl_2.6H_2O$	2.19	2.40	+ 9.4%	(0.252) 0.32
DRH-04-87 B (7-11)	$NiCl_2$(dppp)	0.587	0.589	+0.5%	(0.252) 0.12 – 0.50
DRH-04-87 C (12 – 16)[b]	$Ni(OAc)_2.4H_2O$	2.23	2.72	+21.7%	(0.252) 0.50

[a] Mass of Ni complex weighed out independently (so unknown at the point of calculation and determination. [b] Concentration determined from 1 data point.

6. ICP methodology and results

200 or 500 µL of Ni solution following electrolysis was aliquoted into acid-leached teflon digestion tubes. HCl (1.00 mL, 37%, certified AR grade, supplied by Fisher Chemical™) and HNO_3 (1.50mL, 70%, certified AR grade, supplied by Fisher Chemical™) were added. Samples were digested in an Anton-Paar Multiwave Go Plus with microwave irradiation, ramp rate 18 ° C min^{-1}, ultimate temperature 180 ° C, dwell time 15 minutes. Samples allowed to cool and diluted to 25 mL total volume ultrapure water (Milli-Q type 1 ultrapure water system supplied by Merck). Analysis was completed with an Agilent ICP-OES 5800 VDV spectrometer. Working standard solutions were prepared from commercial reference standard CCS-6 supplied by inorganic ventures, traceable to NIST certified reference materials. All working standards were matrix matched to the digestion media. Ni analysis was completed at 231.694 nm, with internal standard Y 371.029 nm. Measurements were made in axial configuration, plasma flow 12.0 L min^{-1}, auxiliary flow 1.00 L min^{-1}, RF power 1.20 kW.

The unknown metal flakes (recovered from electrodes in DRH-04-58) were tested with semi quantitative screening for unknown metals and confirmed to be Ni. Comparison of ICP and LC-MS quantities is shown in Table .

Table S5: Summary of ICP results and comparison with [Ni] concentrations determined by the LC method.

Sample	Ni 231.604 nm / ppm	[Ni] / mM	[Ni] / mM (LC method)	Solvent system (density / g mL^{-1})
DRH-04-56 (batch recovery, $NiBr_2(PPh_3)_2$, K_3PO_4)	<LOQ	<LOQ	1.61	MeCN/H_2O (0.848)
DRH-04-58 (batch recovery, $NiBr_2(PPh_3)_2$, PPh_4Br)	170.68	2.91	3.22	MeCN/H_2O (0.848)
DRH-04-65	587.44	10.01	8.80	1,4-dioxane/H_2O (1.00)

(batch recovery, $NiBr_2(PPh_3)_2$, PPh_4Br)				
DRH-04-67-4 (flow recovery, $NiBr_2(PPh_3)_2$, 0.050 mL min^{-1})	99.39	1.69	3.19	MeCN/H_2O (0.848)
DRH-04-68-2 (flow recovery, $NiBr_2(PPh_3)_2$, 0.100 mL min^{-1})	294.28	5.01	6.89	MeCN/H_2O (0.848)
DRH-04-69-2 ($NiCl_2$(dppp) catalysed SMCC mixture after flow recovery)	294.84	5.02	4.78	1,4-dioxane/H_2O (1.00)
DRH-04-77 STOCK (NiCl(o-tolyl)$(PPh_3)_2$ catalysed SMCC mixture before recovery)	243.03	4.14	0.66	MeCN/H_2O (0.848)
DRH-04-77-FRACTION (NiCl(o-tolyl)$(PPh_3)_2$ catalysed SMCC mixture after flow recovery)	30.15	0.51	0.67	MeCN/H_2O (0.848)

DRH-04-75 (flow recovery, $NiCl_2$(dppp), 0.075 mL min^{-1})	99.79	1.70	2.49	MeCN/H_2O (0.848)
DRH-04-76 (flow recovery, $NiCl_2$(dppp), 0.075 mL min^{-1})	453.06	7.72	7.25	1,4-dioxane/H_2O (1.00)
PROC BLANK	0.01	0.01	-	-

7. Cyclic Voltammograms of relevant compounds

To a Schlenk-adapted Asynt ElectroReact® with glassy carbon working electrode, platinum rod counter-electrode and silver wire pseudo-reference electrode was added $^{n}Bu_4NPF_6$ (490 mg), sublimed ferrocene (Fc) (1.8 mg) internal standard and nickel/phosphine species (approximately 10 mg). The vessel was evacuated and backfilled with nitrogen three times prior to addition through a septum of acetonitrile (dry, degassed, 15 mL). A cyclic voltammogram was collected using a Metrohm Autolab potentiostat with potential window described below for each voltammogram at a scan rate of 230 mV s^{-1}. Data analysis was conducted using the Nova 2.1.6 software and OriginPro 2023b.

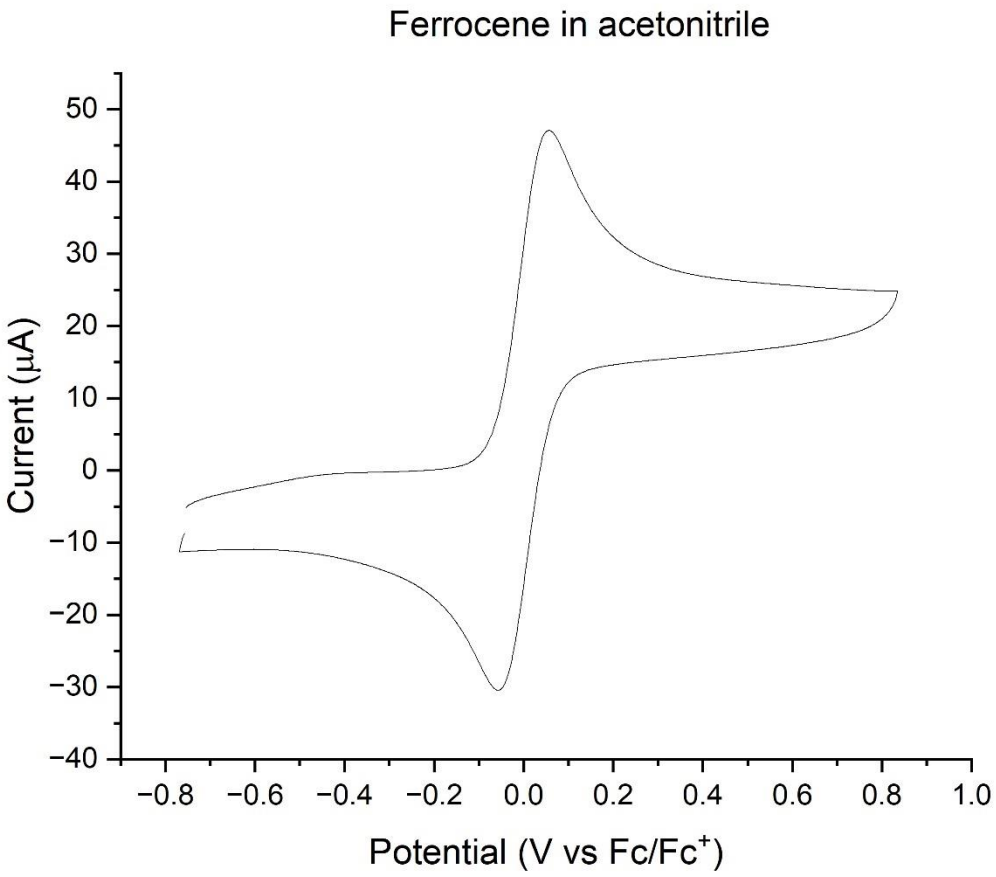

Figure S15: Reference cyclic voltammogram of ferrocene in acetonitrile compared to a Fc/Fc^+ redox process.

Lab book ref. RMW-2-Ni-1/2

7.1. $NiCl_2(dppp)$ (4)

Applied potential = -1.5 to + 1.5 V

Oxidation event at -0.557 V *vs* Fc/Fc^+

Reduction event at -0.957 V *vs* Fc/ Fc^+

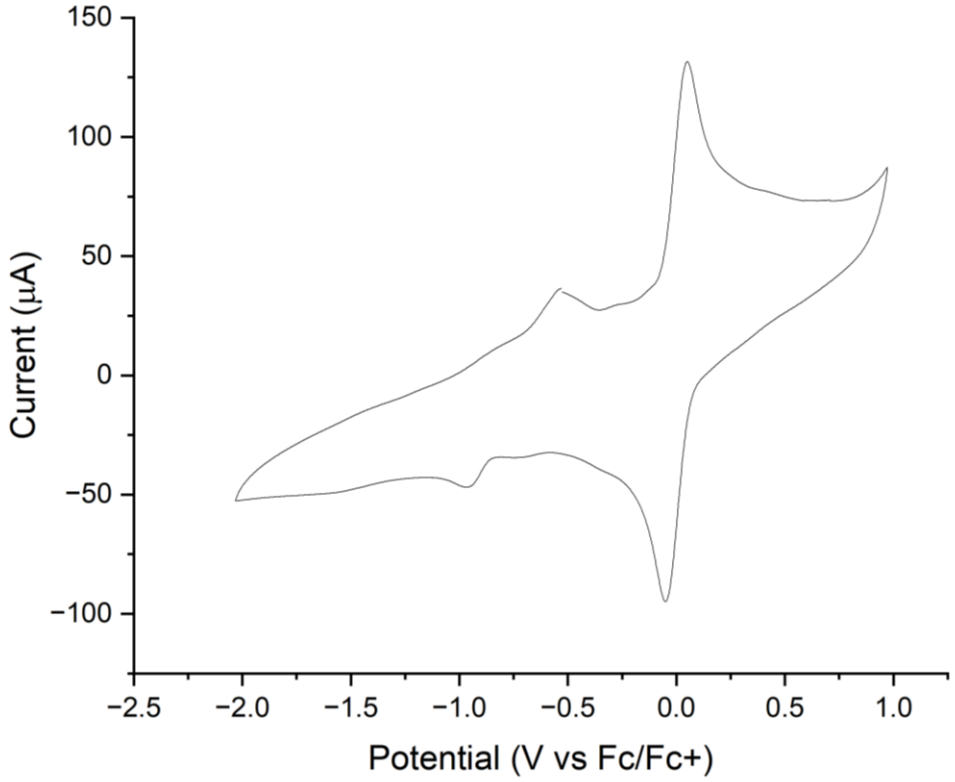

Figure S16: Cyclic voltammogram of $NiCl_2(dppp)$ in acetonitrile compared to a Fc/Fc^+ redox process.

7.2. $NiBr_2(PPh_3)_2$

Applied potential = -1.5 to + 1.5 V

Oxidation event at -0.5114 V *vs* Fc/Fc^+

Reduction event at -0.946 V *vs* Fc/ Fc^+

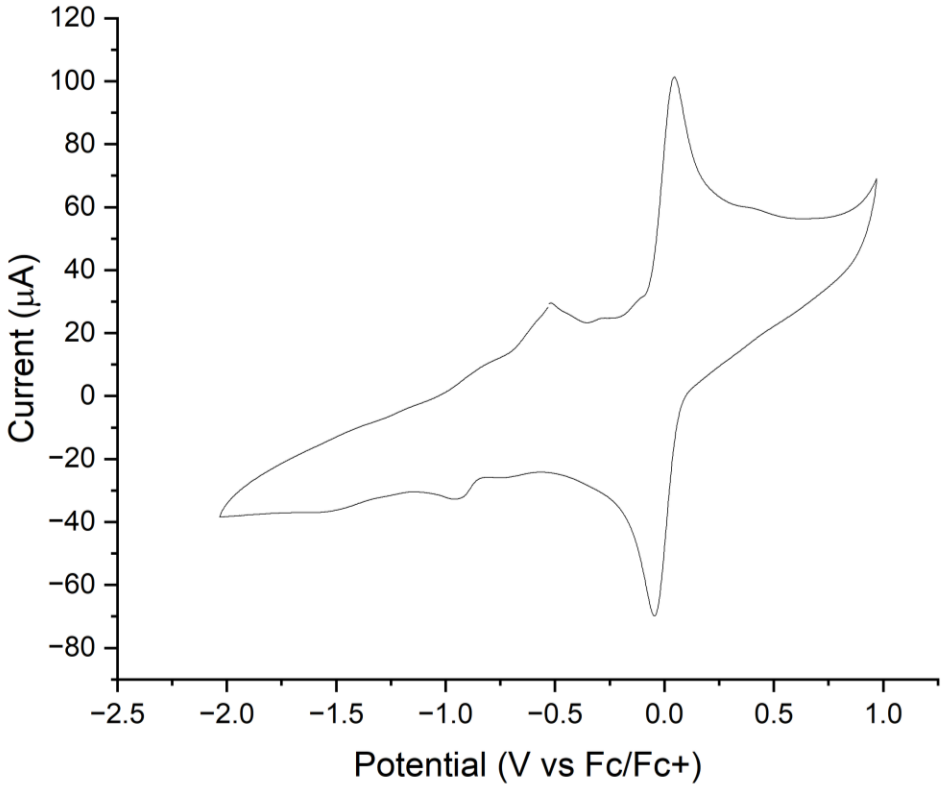

Figure S17: Cyclic voltammogram of $NiBr_2(PPh_3)_2$ in acetonitrile compared to a Fc/Fc^+ redox process.

7.3. NiCl(*o*-tolyl)(PPh_3)$_2$ (5)

(Note: NiCl(*o*-tolyl)(PPh_3)$_2$ exhibited poor solubility in the acetonitrile solvent)

Applied potential = -1.5 to + 1.5 V

Oxidation event at -0.534 V *vs* Fc/ Fc^+

Reduction event at -0.949 V *vs* Fc/ Fc^+

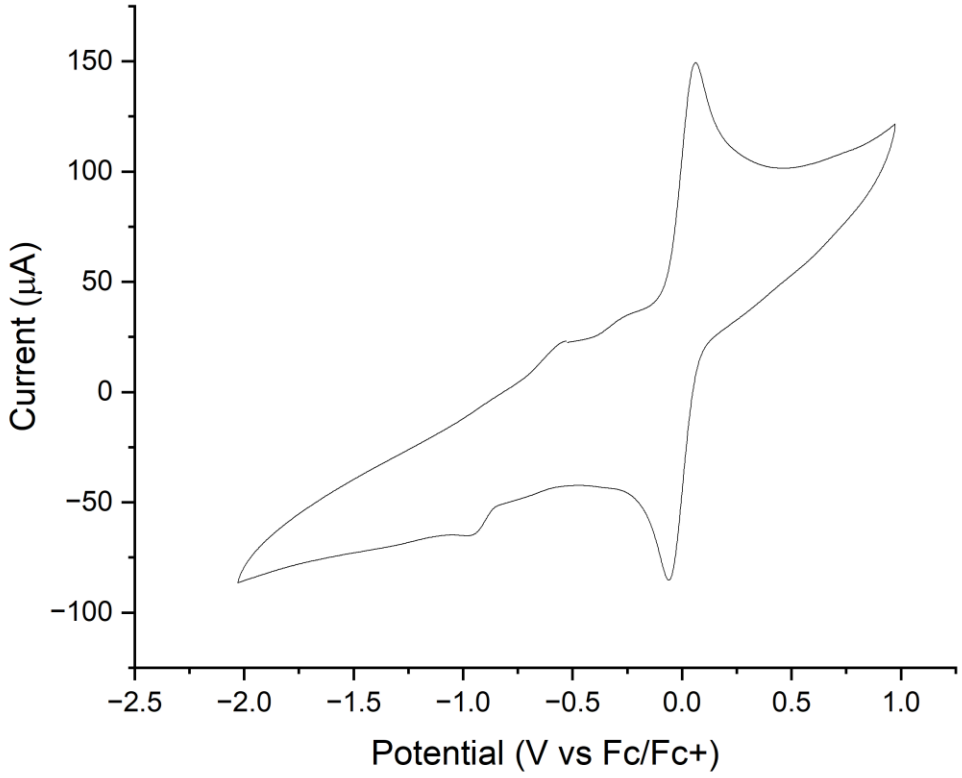

Figure S18: Cyclic voltammogram of NiCl(*o*-tolyl)(PPh_3)$_2$ in acetonitrile compared to a Fc/Fc^+ redox process.

7.4. 1,3-Bis(diphenylphosphino)propane (dppp)

Applied potential = -2.0 to + 2.0 V

Broad oxidation event at 0.5681 V *vs* Fc/Fc^+

Secondary oxidation event at -0.9114 V *vs* Fc/Fc^+

Broad reduction event at -2.1565 V *vs* Fc/Fc^+

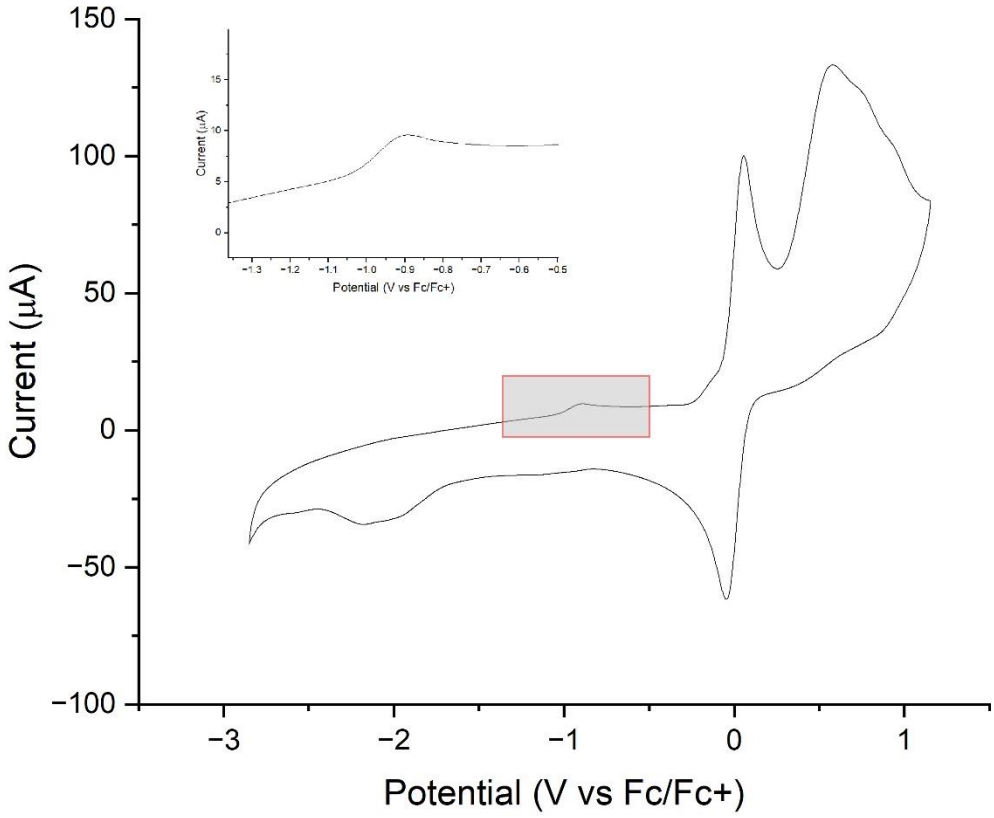

Figure S19: Cyclic voltammogram of dppp in acetonitrile (with magnified region for the oxidation event) compared to a Fc/Fc^+ redox process.

7.5. Triphenylphosphine

Applied potential = -1.5 to +2.5 V

Oxidation events at: 0.7954 V *vs* Fc/Fc^+, 1.3816 V *vs* Fc/Fc^+

Reduction event at -1.8142 V *vs* Fc/Fc^+

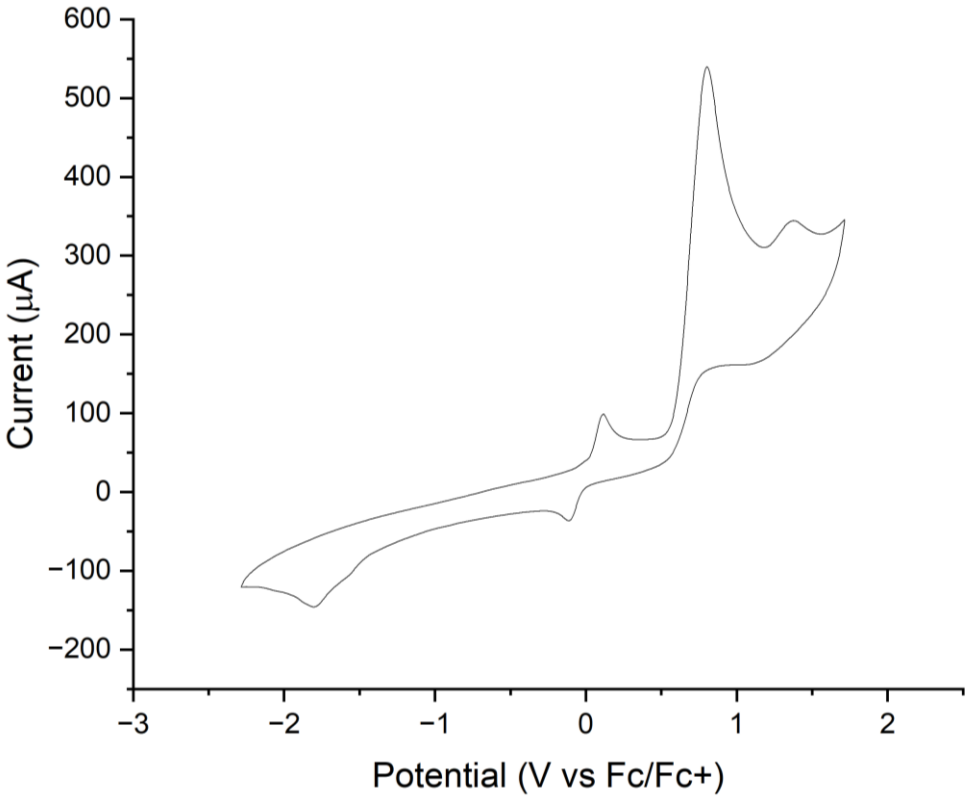

Figure S20: Cyclic voltammogram of PPh_3 in acetonitrile compared to a Fc/Fc^+ redox process.

8. Batch electrochemical recovery of Ni

8.1. Methodology

To a Asynt ElectroReact® fitted with a stainless steel (SS) cathode and graphite anode, a known quantity of $NiBr_2(PPh_3)_2$ and electrolyte (either K_3PO_4 or PPh_4Br) was added, followed by solvent. A constant potential difference was applied across the electrodes, and the mixture was stirred at 700 rpm at room temperature for a given time. Afterwards, direct aliquots (5 – 50 µL) of the mixture were taken and analysed by the LC method for Ni content. After determining the concentration of Ni in solution following electrolysis, the known initial concentration of Ni was used to calculate a % Ni recovery by electrochemical means. The reaction mixtures were later analysed by ICP elemental analysis and quantification to verify the LC method of Ni determination. The results are summarised in Table S6.

Table S6: Summary of electrochemical recovery experiments.

Lab book ref.	DRH-04-56	DRH-04-58	DRH-04-65
Compound	$NiBr_2(PPh_3)_2$ 212 mg, 0.285 mmol	$NiBr_2(PPh_3)_2$ 180 mg, 0.242 mmol	$NiBr_2(PPh_3)_2$ 197 mg, 0.265 mmol
Electrolyte	K_3PO_4 196 mg, 0.923 mmol (3.2 equiv.)	PPh_4Br 237 mg, 0.565 mmol (2.3 equiv.)	PPh_4Br 460 mg, 1.097 mmol (4.1 equiv.)
Solvent	MeCN/H_2O (75:25 v/v), 14.1376 g	MeCN/H_2O (75:25 v/v), 13.5850 g	1,4-dioxane/H_2O (75:25 v/v), 21.9699 g
Constant potential difference / V	4.0	2.5	3.3
Reaction time / h	16	16	6
Initial concentration of [Ni] / mM	17.11	15.13	12.06
End concentration of [Ni] (LC method) / mM	1.59	3.05	8.80

End concentration of [Ni] (ICP) / mM	<LOQ	2.91	10.01
% Ni recovery	90.7%	79.8%	27.1%
([Ligand] / mM)	(0.268)	(0.271)	(0.319)
[Ligand]/[Ni] ratio range	0.22 – 0.52	0.11 – 0.41	0.15 – 0.29

8.2. Batch Electrochemical recovery of Ni from $NiBr_2(PPh_3)_2$ using K_3PO_4

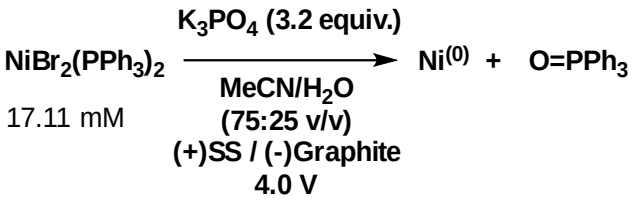

Recovery of Ni from $NiBr_2(PPh_3)_2$ using K_3PO_4 as an electrolyte, MeCN/H_2O (75:25 v/v) as the solvent. SS (+ve), Graphite (-ve) electrodes, 4.0 V (constant voltage), 16 mA (initial current) 16 h, 700 rpm stirring.

A phase partition was observed, likely caused by the K_3PO_4 electrolyte. It should be noted that not all of the solids dissolved in the reaction medium, and after the reaction a large quantity of black particulate matter was observed both on the electrodes and at the bottom of the vessel (Figure S18-S20). This was speculated to be Ni colloids.

Starting concentration Ni = 17.11 mM
End concentration Ni (LC method) = 1.59 mM
% Ni recovery = 90.7%

(LCMS data lab book ref. DRH-04-60 D 6 to 13)

ICP showed sample less than limit of quantification.

Figure S21: Graphite electrode (anode) and reaction mixture from the ElectroReact.

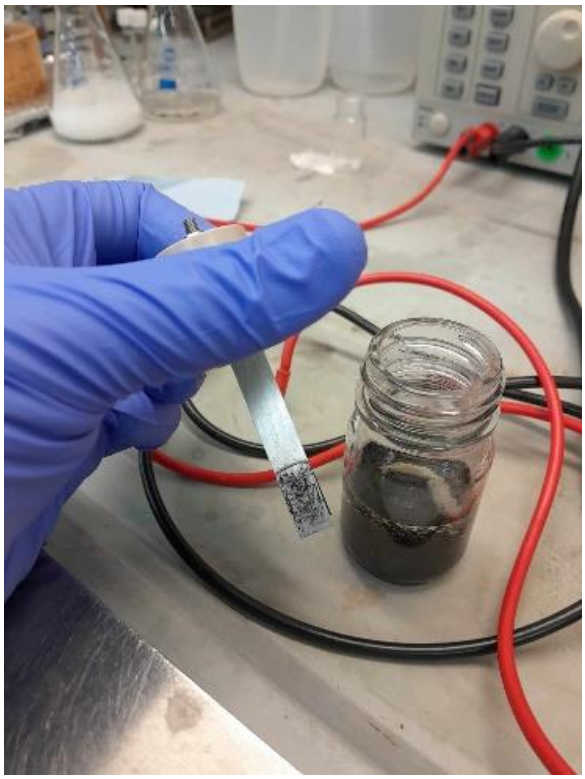

Figure S22: Stainless steel electrode (cathode) with black Ni particulate matter deposited on the surface.

Figure S23: ElectroReact reaction mixture containing a biphase and a large quantity of black particulate matter.

Lab book ref. DRH-04-56

8.3. Batch Electrochemical recovery of Ni from $NiBr_2(PPh_3)_2$ using PPh_4Br

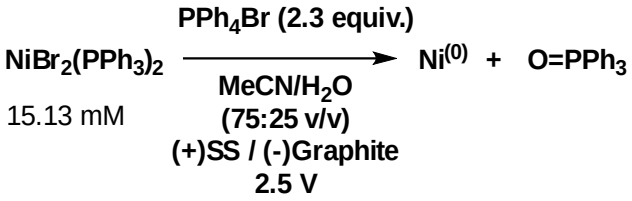

Recovery of Ni from $NiBr_2(PPh_3)_2$ using PPh_4Br as an electrolyte, MeCN/H_2O (75:25 v/v) as the solvent. SS (+ve), Graphite (-ve) electrodes, 2.5 V (constant voltage), 7 mA (initial current) 16 h, 700 rpm stirring.

Over time, green solid formed on the SS electrode (Figure S22) and the current fell to 4 mA (after 2 h). After 3.5 h, the solution had turned yellow (Figure S21), likely from Br_2 formation from electrolyte or complex degradation, and the current had dropped to 2 mA. After 16 h, the current was 0 mA and the reaction had halted (significant plating on SS electrode likely caused the fall in current).

Starting concentration Ni = 15.13 mM
End concentration Ni (LC method) = 3.05 mM
% Ni recovery = 79.8%
(LCMS data lab book ref. DRH-04-70 A 1 to 6)

ICP DRH-04-58 170.68 ppm Ni, 2.91 mM

Density of solvent = 0.848

ICP confirmed that the recovered metal from the electrodes was Ni.

Figure S24: ElectroReact after electrochemical recovery of Ni. The yellow solution is proposed to be due to the generation of Br_2.

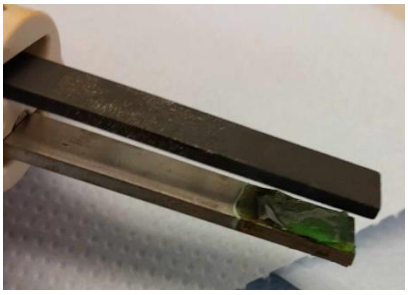

Figure S25: Black and green plated deposits on the stainless steel electrode (cathode)

Lab book ref. DRH-04-58

8.4 Identity of the recovered Ni compound

The identity of the green electrode deposits was examined in further detail in repeat reactions (lab book refs. DRH-04-58-2 (aerobic conditions, powdered, not dried), DRH-04-58-3 (aerobic conditions, powdered, dried), DRH-04-58-4 (anaerobic conditions, powdered, dried)). Initially, FTIR was used to probe the identity of powdered flakes of the green material (the flakes were powdered after washing with deionised water to remove any surface contaminants). Potential matches of NiO (a dark green solid, insoluble in water) and $NiBr_2.3H_2O$ (a yellow-orange solid, soluble in water) were tested.

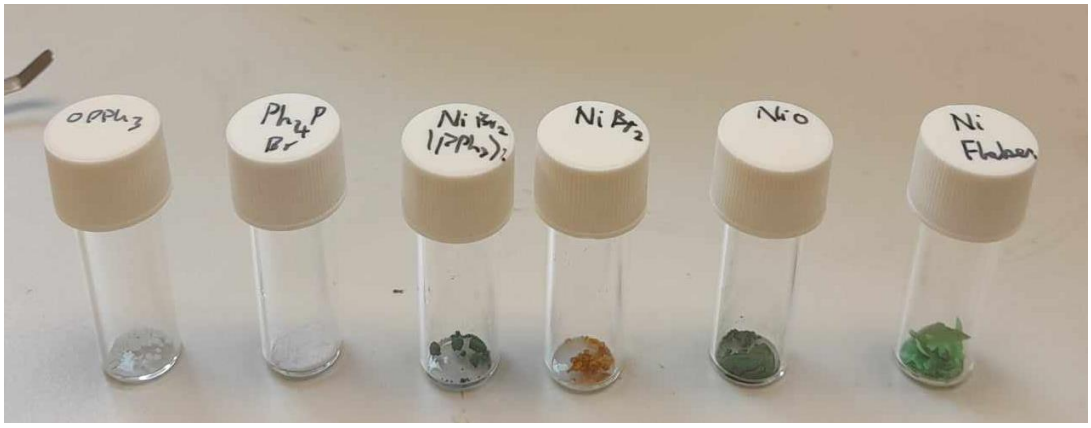

Figure S26: Samples of potential components in the recovered Ni flakes. Left to right: triphenylphosphine oxide, tetraphenylphosphonium bromide (PPh_4Br), $NiBr_2(PPh_3)_2$, $NiBr_2.3H_2O$, nickel (II) oxide (NiO), recovered Ni flakes (DRH-04-58-2).

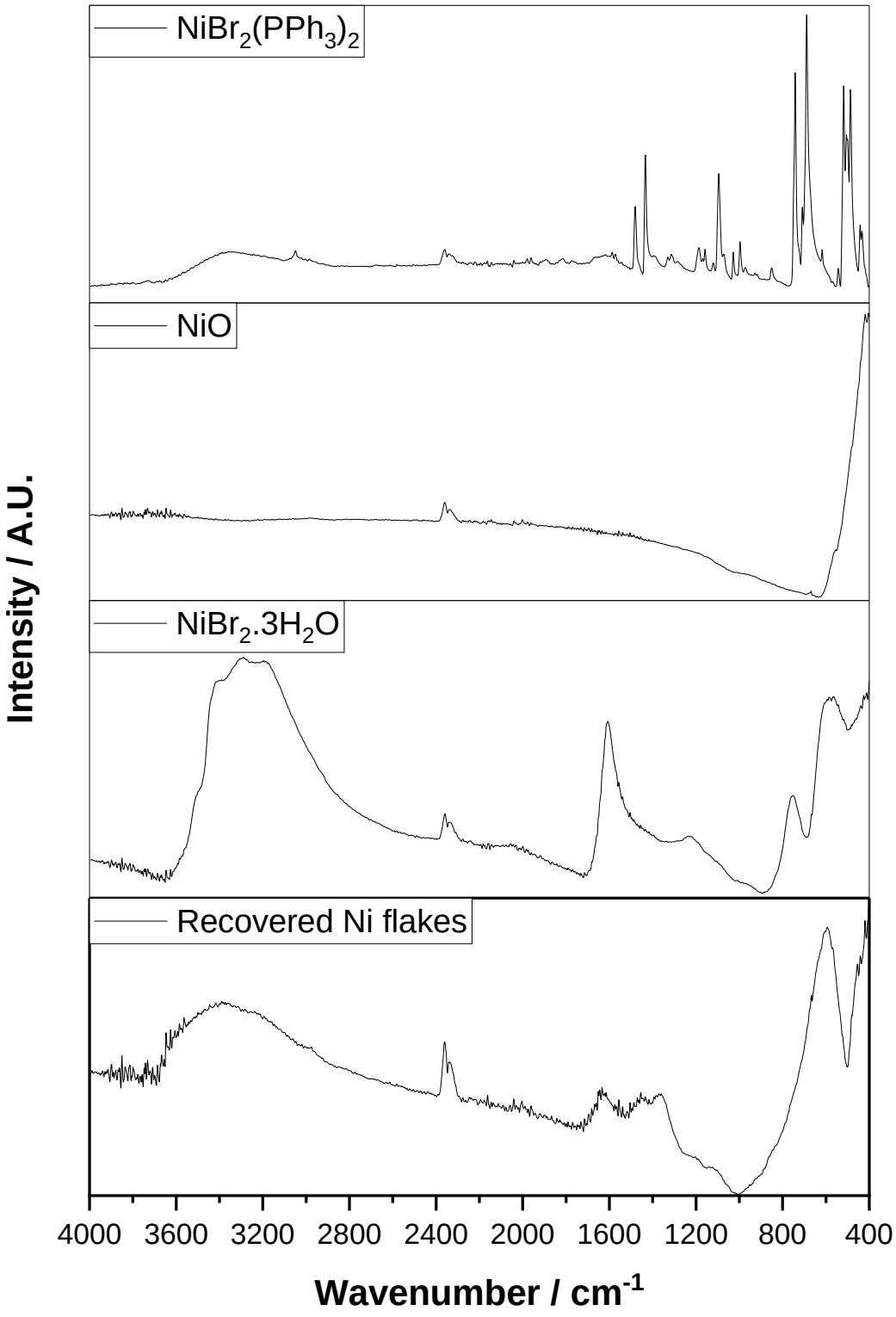

Figure S27: FTIR spectra of the recovered Ni flakes (bottom) and potential Ni compounds.

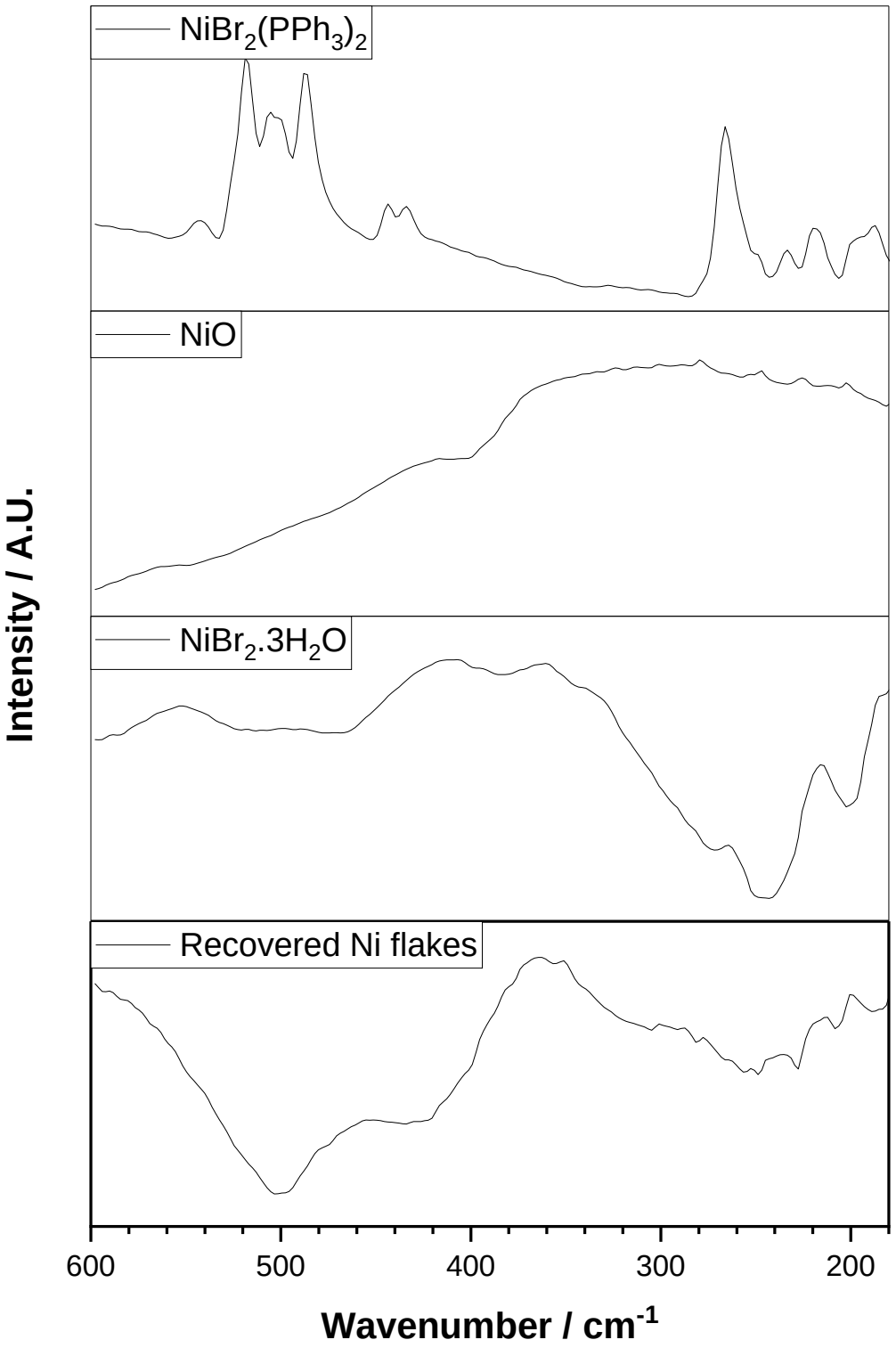

Figure S28: FTIR (FarIR) spectra of the recovered Ni flakes (bottom) and potential Ni compounds.

Although it is not conclusive, features of both NiO and $NiBr_2.3H_2O$ are present, with $NiBr_2.3H_2O$ looking like a closer match. This finding was replicated by the use of FarIR to examine low-wavenumber vibrations.

Powder XRD was deployed next to determine a crystal structure match on a dried sample of the recovered Ni flakes (DRH-04-59-3). However, as can be seen from the trace, the powdered sample was largely amorphous with extremely broad peaks, so it was not possible to identify a probable match.

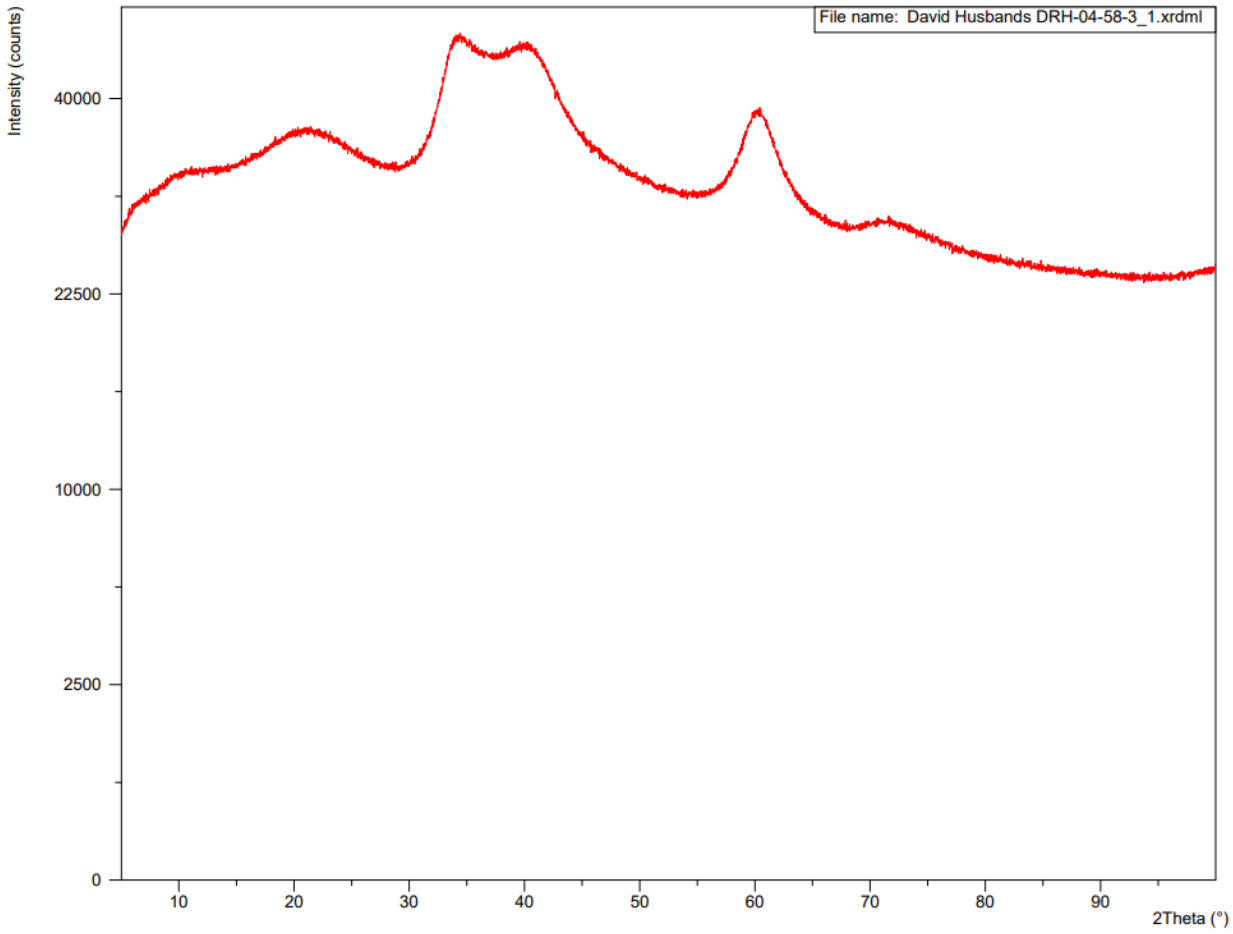

Figure S29: Powder X-ray diffraction (pXRD) spectrum of recovered Ni flakes (powdered, dried, DRH-04-58-3)

Ion chromatography (IC) was then used to identify a Br^- counterion (if one was present). On a weight of 1.8488 mg of recovered Ni flakes (DRH-04-58-2), Br was present in 0.5322 ppm (effectively trace). It is unclear whether this is from $NiBr_2$ or from residual electrolyte (PPh_4Br).

As a complimentary test for bromide, a silver nitrate ($AgNO_3$) test was carried out. A sample of the powdered flakes (DRH-04-58-2) were added to deionised water (~0.5 mL) and sonicated. Interestingly, the green powder appeared to be completely insoluble in water, even with sonication, which would be counter to $NiBr_2$ being the identity of the solid (NiO is insoluble in water). Upon addition of the supernatant to a solution of $AgNO_3$ in water, a light turbidity was observed, indicating the presence of Br^-. However, it should be noted one more that it is unclear whether this is from $NiBr_2$ or from residual electrolyte (PPh_4Br).

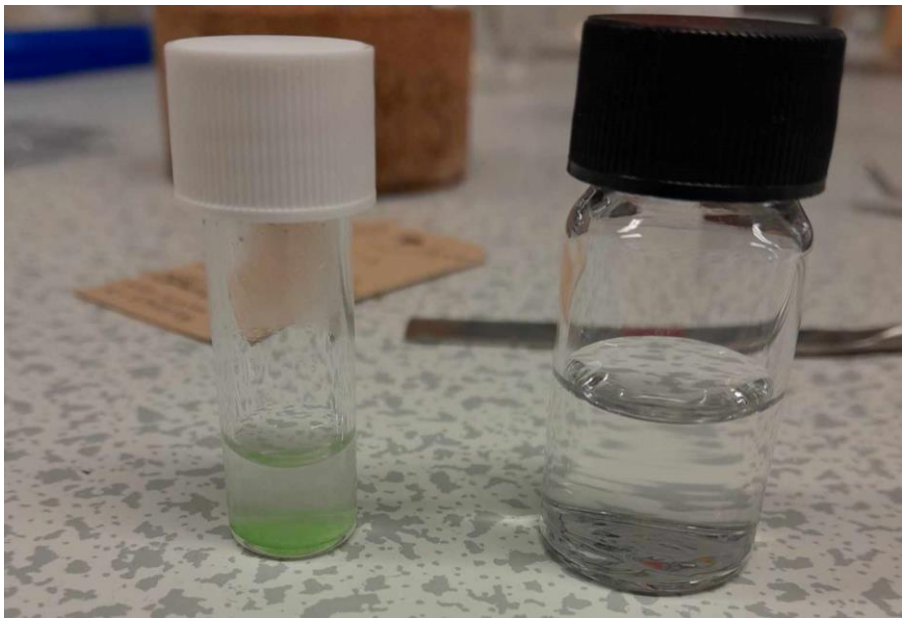

Figure S30: (left) sonicated sample of powdered recovered Ni flakes in water, (right) $AgNO_3$ solution

Figure S31: (left) $AgNO_3$ solution, (right) $AgNO_3$ solution after addition of supernatant from powdered Ni flakes sample. Note the light turbidity indicating the presence of bromide ions (as AgBr).

A sample of the powdered recovered flakes were dried (DRH-04-58-3) (by heating with a heatgun for 1 min, then under vacuum for 24 hours) to remove any residual solvent (mass loss = 8.1 mg, 28%).

A second sample of the electrochemical recovery reaction done anaerobically under a flow of N_2 was also obtained and dried in the same manner (DRH-04-58-4), turning from pale green to black (mass loss = 10.0 mg, 44%)

Figure S32: Electrochemical recovery setup (using quantities from Section 8.3) under a flow of N_2

Figure 1: Reaction after electrochemical recovery (DRH-04-58-4). Note the green Ni compounds deposits alongside the black spots, possibly of Ni nanoparticles.

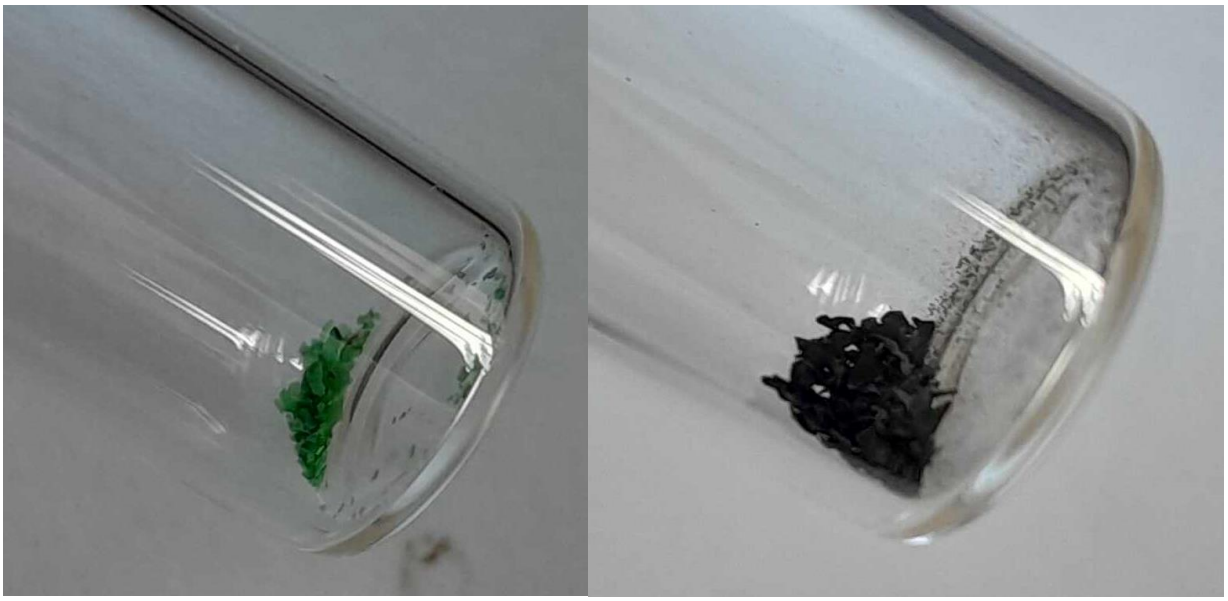

Figure S34: (left) sample of powdered Ni flakes (anaerobic) before drying, (right) sample of powdered Ni flakes (anaerobic) after drying

ICP analysis of the two samples revealed that the anaerobic dried flakes have a much higher Ni content than the aerobic dried flakes. The most likely identity of the anaerobic flakes is of Ni_2O_3 (by % Ni), which would be consistent with heating an unstable Ni compound in air (additionally, Ni_2O_3 is a black solid). This is complimented by IR done on the samples, which match closely to NiO.

In contrast, the aerobic dried flakes have a lower Ni content, which could be due to an intractable mixture of NiO with other compounds ($NiBr_2$, and more likely intercalated solvent). This would explain the relatively high % Ni, alongside the insolubility of the sample in water (a feature of NiO), and the low availability of Br for the $AgNO_3$ test. Irremovable solvent is more likely the cause, as only trace Br was found by ion chromatography.

Table S7: ICP results on the recovered Ni samples, and potential identities for Ni in the samples.

Sample	% Ni (by ICP)
DRH-04-58-3 (aerobic, dried recovered flakes) Green powder	58.1
DRH-04-58-4 (anaerobic, dried recovered flakes)	70.9

Black powder	

Potential compound identities	**Theoretical % Ni**
$NiBr_2$	26.86
NiBr2.3H2O	21.54
NiO	78.58
Ni_2O_3 ($Ni^{(III)}$ oxide)	70.89
Ni nanoparticles	100

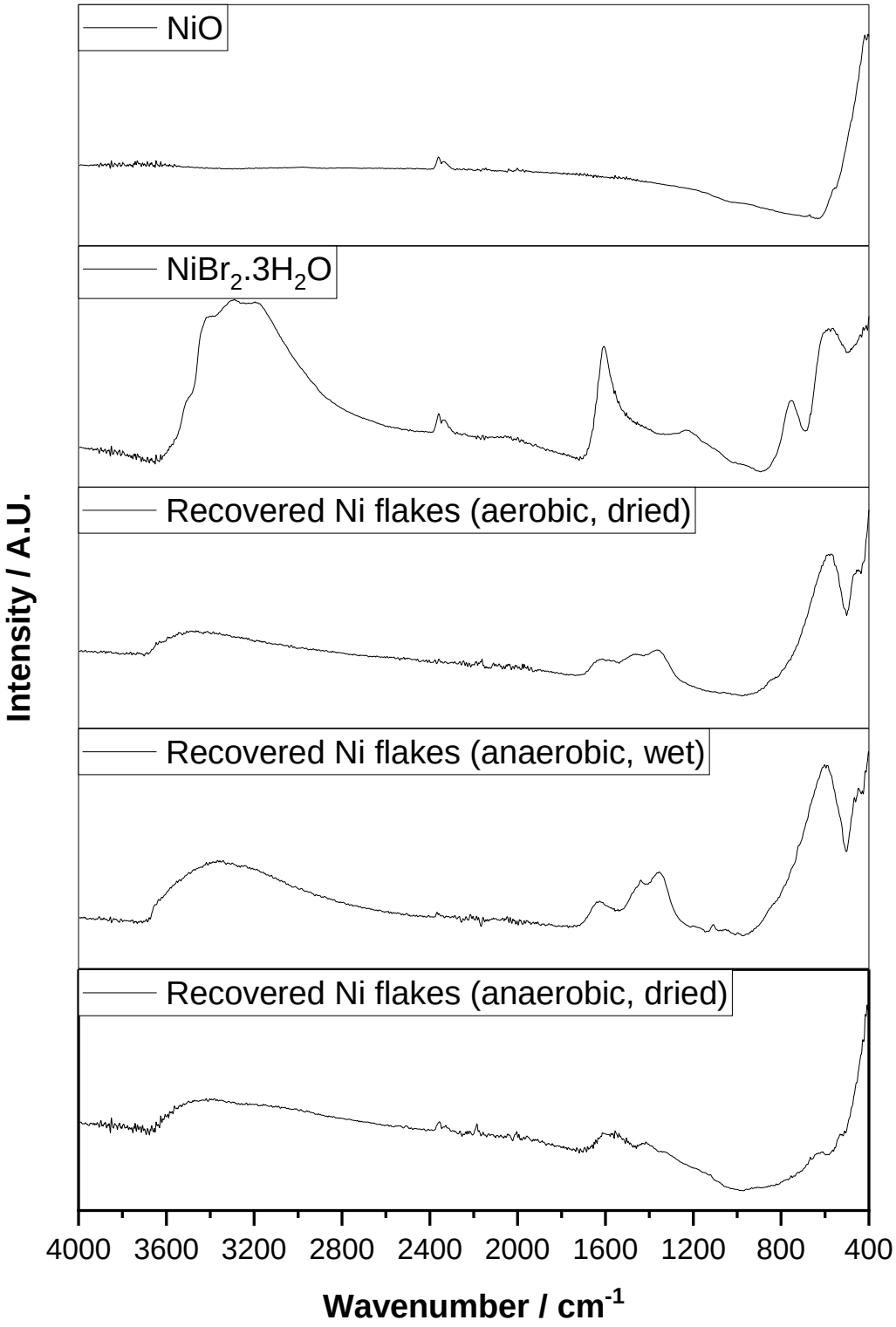

Figure S35: FTIR spectra of the recovered Ni flakes and potential Ni compounds.

In the light of evidence we have gathered, it seems plausible that the majority of the green deposits collected are nickel oxides (NiO, Ni_2O_3) as they are insoluble, match closely with ICP values, and the anaerobic Ni recovery IR closely resembles NiO. There are likely small quantities of $NiBr_2$ (IC, $AgNO_3$ test, IR) present under aerobic conditions, although it is challenging to rule out residual electrolyte (PPh_4Br) as the source. The lower than expected % Ni for aerobic recovery could be due to intercalated solvent and electrolyte, which is not easily removed. Further work and specialist techniques which we do not have access to, such as microscopy will be required to fully confirm this hypothesis.

8.5 Batch Electrochemical recovery of Ni from $NiBr_2(PPh_3)_2$ using dioxane solvent

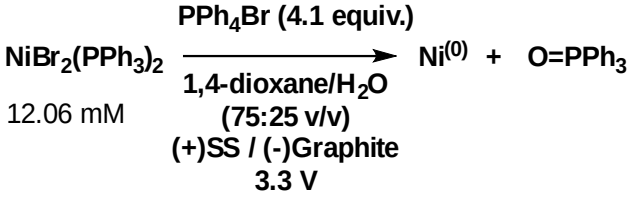

Recovery of Ni from $NiBr_2(PPh_3)_2$ using PPh_4Br as an electrolyte, 1,4-dioxane/H_2O (75:25 v/v) as the solvent. SS (+ve), Graphite (-ve) electrodes, 3.3 V (constant voltage), 3 mA (initial current) 6 h, 700 rpm stirring.

Over time, green deposits on the SS electrode were observed (after 1.25 h). After 6 h, the reaction mixture was yellow with black deposits and 0 mA current was observed, so the reaction was halted.

Starting concentration Ni = 12.06 mM
End concentration (LC method) Ni = 8.80 mM
% Ni recovery = 27.1%

(LCMS data lab book ref. DRH-04-70 B 7 to 12)

ICP showed 547.44 ppm, 10.01 mM

Density of solvent = 1.00

Lab book ref. DRH-04-65

9. Flow electrochemical recovery of Ni

9.1. Flow electrochemical recovery setup

A miniaturised electrochemical flow reactor[12,13] was assembled (Figure S23) containing alternating PTFE spacers and electrodes (in the order; steel top, PTFE blank, stainless steel (SS) cathode, PTFE flow channel, graphite anode, PTFE flow channel, SS cathode, PTFE blank, steel bottom). Each component had a thickness of 1 mm, and the two PTFE flow channels had a volume of 0.464 mL, giving an overall reactor volume of 0.928 mL. The two SS electrodes were wired in parallel. The reactor was flushed with deionised water (5 mL) followed by acetonitrile (5 mL) at a rate of 1 mL min^{-1} to check for leaks. A stock solution (approx. 5 mL) of Ni complex and PPh_4Br electrolyte was prepared in a solvent mixture and charged into a 10 mL glass gas-tight syringe. Using a syringe pump (Figure), 1 mL of stock solution was flushed through the reactor at a rate of 1 mL min^{-1}. A constant potential difference was applied, and the stock solution was pumped through the reactor at a constant flow rate. After a further 2 mL of stock solution had passed through the reactor (approximately 2 residence times to allow for steady state to be achieved), a fraction (approximately 1 mL) was collected. This fraction was aliquoted directly (5 – 50 µL) and analysed by the LC method for Ni content. The same fractions were later analysed by ICP elemental analysis and quantification to verify the LC method of Ni determination. After determining the concentration of Ni in solution after electrolysis, the known initial concentration of Ni was used to calculate a % Ni recovery by electrochemical means.

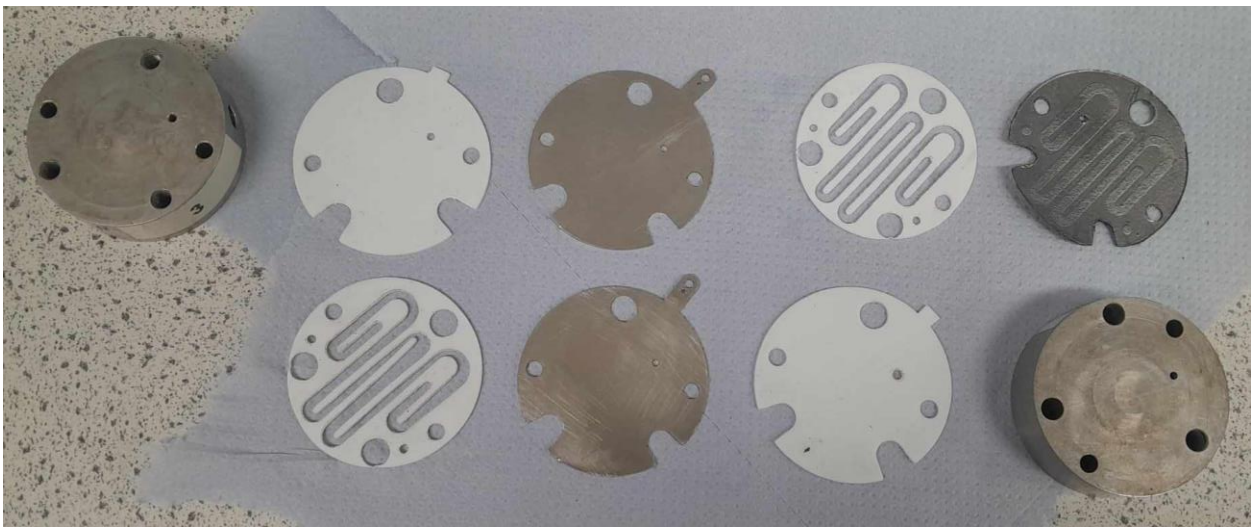

Figure S36: Reactor components. 2x stainless steel (SS) electrodes and 1x graphite electrode. 2 PTFE spacers (1 mm thickness) were used, each with a flow channel volume of 0.464 mL. This gave an overall reactor volume of 0.928 mL.

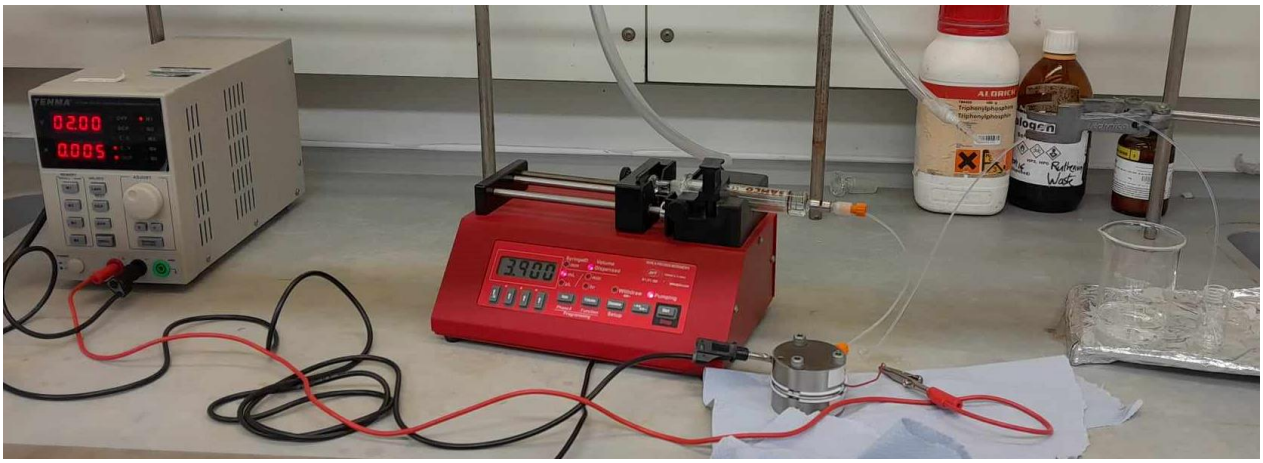

Figure S37: Electrochemical flow reactor setup.

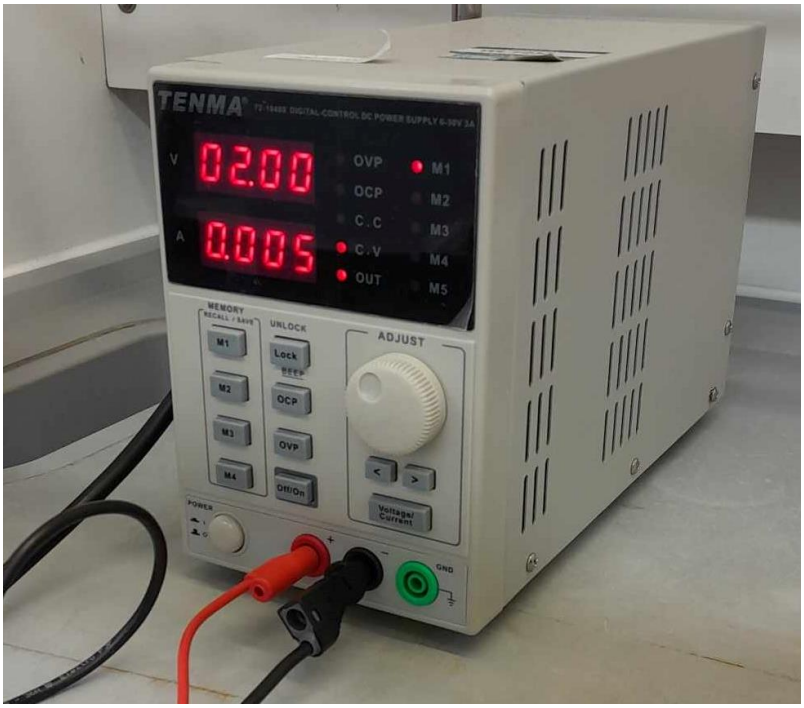

Figure S38: Powerpack for electrochemistry. A constant voltage was kept during the reaction.

Figure S39: Syringe pump and flow reactor.

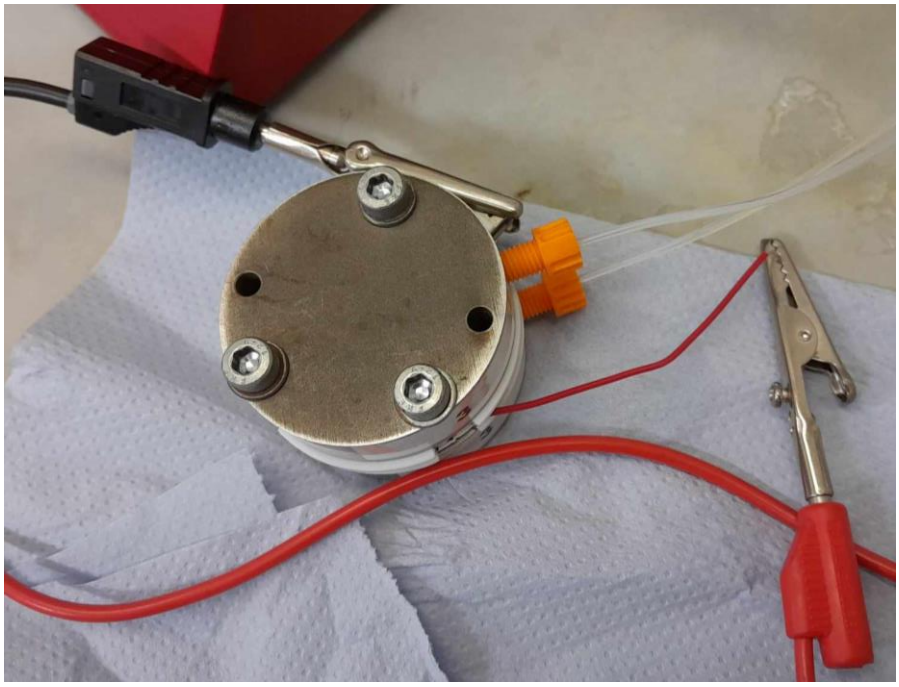

Figure S40: Reactor setup. Red wire = graphite anode, black wire = SS cathode. Inlet is on top, outlet from bottom.

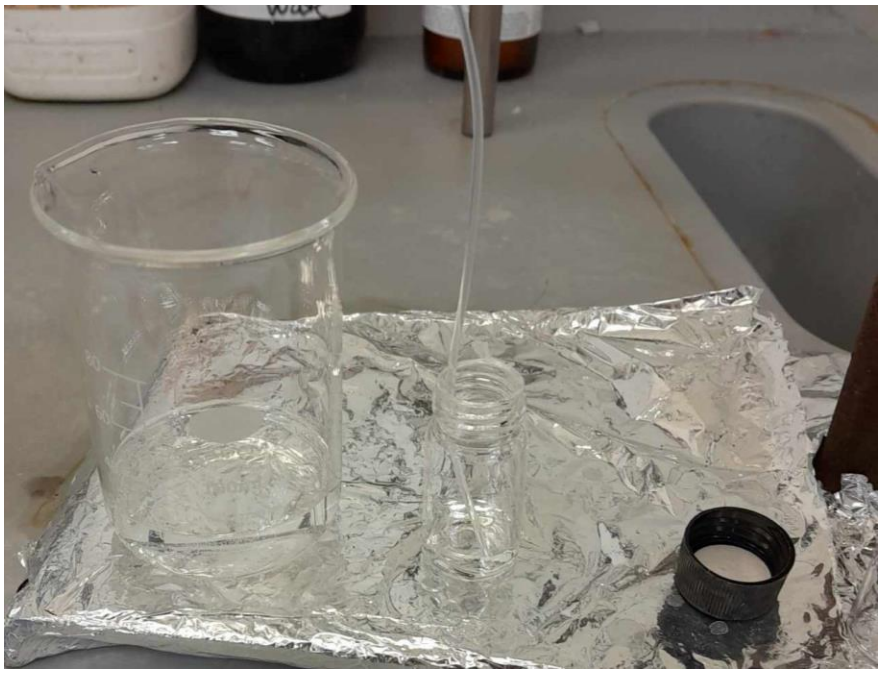

Figure S41: Waste beaker and collection vial.

Table S8: Summary of flow electrochemical recovery of Ni from stock solutions.

Lab book ref.	DRH-04-67	DRH-04-68	DRH-04-75	DRH-04-76
Compound	$NiBr_2(PPh_3)_2$ 156 mg, 0.210 mmol	$NiBr_2(PPh_3)_2$ 156 mg, 0.210 mmol	$NiCl_2(dppp)$ 47 mg, 0.0871 mmol	$NiCl_2(dppp)$ 47 mg, 0.0871 mmol
Electrolyte	PPh_4Br 300 mg, 0.716 mmol (3.4 equiv.)	PPh_4Br 300 mg, 0.716 mmol (3.4 equiv.)	PPh_4Br 148 mg, 0.353 mmol (4.1 equiv.)	PPh_4Br 147 mg, 0.351 mmol (4.1 equiv.)
Solvent	MeCN/H_2O (75:25 v/v), 8.5376 g	MeCN/H_2O (75:25 v/v), 8.5376 g	MeCN/H_2O (75:25 v/v), 5.0580 g	1,4-dioxane/H_2O (75:25 v/v), 5.6513 g
Constant potential difference / V	2.0	2.0	2.0	2.3

Flow rate / mL min^{-1}	0.050	0.100	0.075	0.075
Initial concentration of [Ni] / mM	20.85	20.85	14.60	15.18
End concentration of [Ni] (LC method) / mM	3.19	5.48	2.43	6.33
End concentration of [Ni] (ICP) / mM	1.69	5.01	1.70	7.72
% Ni recovery	84.7%	73.7%	83.3%	58.3%
([Ligand] / mM) [Ligand]/[Ni] ratio range	(0.271) 0.10 – 0.26	(0.271) 0.11 – 0.41	(0.270) 0.13 – 0.25	(0.315) 0.27 – 0.54

9.2. Flow electrochemical recovery of Ni from $NiBr_2(PPh_3)_2$

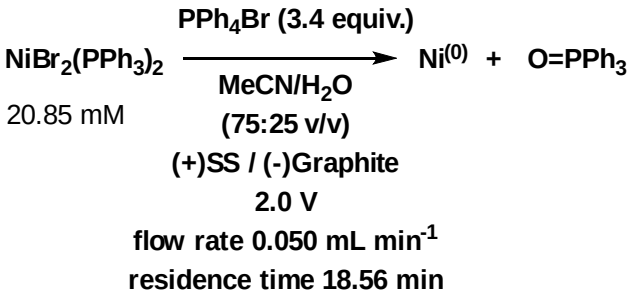

Recovery of Ni from $NiBr_2(PPh_3)_2$ using PPh_4Br as an electrolyte, MeCN/H_2O (75:25 v/v) as the solvent. 2 x SS (+ve, parallel), Graphite (-ve) electrodes, 2.0 V (constant voltage), 19 mA (initial current), flow rate = 0.050 mL min^{-1}, residence time = 18.56 min.

Table S9: Collected fractions from the flow electrochemical recovery of Ni.

Sample number	Collection volume after start of electrochemical recovery / mL
DRH-04-67-1	0.150 – 0.450
DRH-04-67-2	0.450 – 1.000
DRH-04-67-3	1.000 – 2.000
DRH-04-67-4	2.000 – 3.100

After 10 min, the current fell to 4 mA and stayed constant. The colour of the collected fractions turned yellow (likely from Br_2 formation from electrolyte or complex degradation). Green deposits were seen on the SS electrodes, similar to the batch recovery process.

DRH-04-67-2

Starting concentration Ni = 20.85 mM
End concentration Ni (LC method) = 5.29 mM
% Ni recovery = 74.6%
[Ligand] / mM = 0.252
[Ni]/[Ligand] ratio range = 0.15 – 0.54
(LCMS data lab book ref. DRH-04-87 E 17 to 22)

DRH-04-67-3

Starting concentration Ni = 20.85 mM
End concentration Ni (LC method) = 3.72 mM
% Ni recovery = 82.2%
[Ligand] / mM = 0.271
[Ni]/[Ligand] ratio range = 0.11 – 0.31
(LCMS data lab book ref. DRH-04-70 D 19 to 24)

DRH-04-67-4 (flow reaction at steady state)

Starting concentration Ni = 20.85 mM
End concentration Ni (LC method) = 3.19 mM
% Ni recovery = 84.7%
[Ligand] / mM = 0.271
[Ni]/[Ligand] ratio range = 0.10 – 0.26
ICP 99.39 ppm, 1.69 mM

Density of solvent = 0.848

(LCMS data lab book ref. DRH-04-70 E 25 to 30)

Figure S42: Solutions of $NiBr_2(PPh_3)_2$ in $MeCN/H_2O$. Stock solution before electrolysis (left), then collections throughout the reaction. Note the increasing yellow of the collected samples likely due to the generation of Br_2 in solution.

Figure S43: Stainless steel electrodes (cathode) showing green deposits of Ni metal following the reaction channel.

Lab book ref. DRH-04-67

9.3. Flow electrochemical recovery of Ni from $NiBr_2(PPh_3)_2$ (faster flow rate)

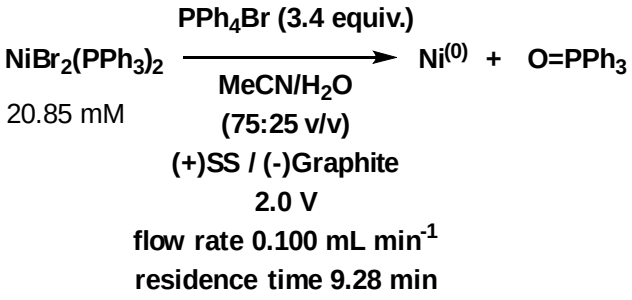

Recovery of Ni from $NiBr_2(PPh_3)_2$ using PPh_4Br as an electrolyte, $MeCN/H_2O$ (75:25 v/v) as the solvent. 2 x SS (+ve, parallel), Graphite (-ve) electrodes, 2.0 V (constant voltage), 15 mA (initial current), flow rate = 0.075 mL min^{-1}, residence time = 9.28 min.

Green deposits on the SS electrode were observed. However, in this case the reaction mixture did not turn yellow.

DRH-04-68-2 (3 mL – 4 mL fraction after start of flow electrochemical recovery. Reaction at steady state)

Starting concentration Ni = 20.85 mM
End concentration Ni (LC method) = 5.48 mM
% Ni recovery = 73.7%
[Ligand] / mM = 0.271
[Ni]/[Ligand] ratio range = 0.11 – 0.41
(LCMS data lab book ref. DRH-04-70 F 31 to 36)

ICP 294.28 ppm Ni, 5.01 mM

Density of solvent = 0.848

Lab book ref. DRH-04-68

9.4. Flow electrochemical recovery of Ni from $NiCl_2$(dppp)

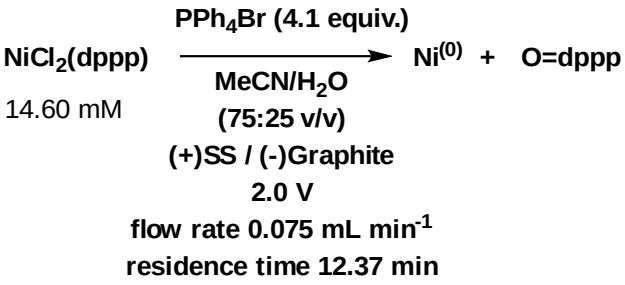

Recovery of Ni from $NiCl_2$(dppp) using PPh_4Br as an electrolyte, MeCN/H_2O (75:25 v/v) as the solvent. 2 x SS (+ve, parallel), Graphite (-ve) electrodes, 2.0 V (constant voltage), 300 mA (initial current), flow rate = 0.075 mL min^{-1}, residence time = 12.37 min.

(DRH-04-75 2 mL – 3 mL fraction after start of flow electrochemical recovery. Reaction at steady state)

Concentration of Ni at the start = 14.60 mM

Concentration of Ni at the end (LC method) = 2.43 mM

% recovery of Ni = 83.3%

[Ligand] / mM = 0.270

[Ni]/[Ligand] ratio range = 0.13 – 0.25

(LCMS data lab book ref. DRH-04-78 A 2 to 7)

ICP Ni 99.79 ppm, 1.70 mM

Density of solvent = 0.848

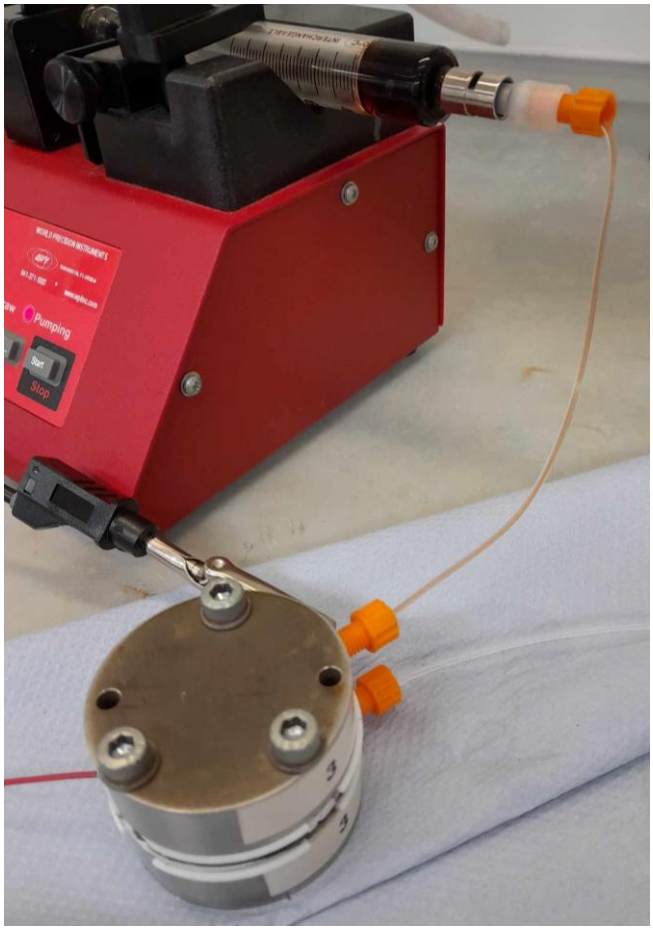

Figure S44: Electrochemical flow reactor showing decolourisation of $NiCl_2$(dppp) solution (MeCN/H_2O)

Figure S45: $NiCl_2$(dppp) solution before (left) and after (right) electrolysis.

Figure S46: Stainless steel (+ve) electrode after electrolysis. Note the orange flakes of Ni compounds deposited along the flow pathway.

Lab book ref. DRH-04-75

9.5. Flow electrochemical recovery of Ni from $NiCl_2$(dppp) from dioxane

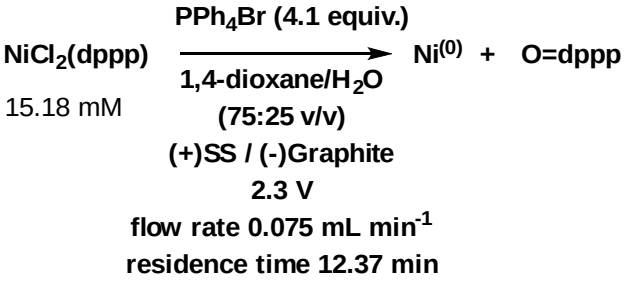

Recovery of Ni from $NiCl_2$(dppp) using PPh_4Br as an electrolyte, 1,4-dioxane/H_2O (75:25 v/v) as the solvent. 2 x SS (+ve, parallel), Graphite (-ve) electrodes, 2.3 V (constant voltage), 12 mA (initial current), flow rate = 0.075 mL min^{-1}, residence time = 12.37 min.

DRH-04-76 (2 mL – 3 mL fraction after start of flow electrochemical recovery. Reaction at steady state)

Concentration of Ni at the start = 15.18 mM

Concentration of Ni at the end (LC method) = 6.33 mM

% recovery of Ni = 58.3%

[Ligand] / mM = 0.315

[Ni]/[Ligand] ratio range = 0.27 – 0.54

(LCMS data lab book ref. DRH-04-78 B 8 to 13)

ICP Ni 453.06, 7.72 mM

Density of solvent = 1.00

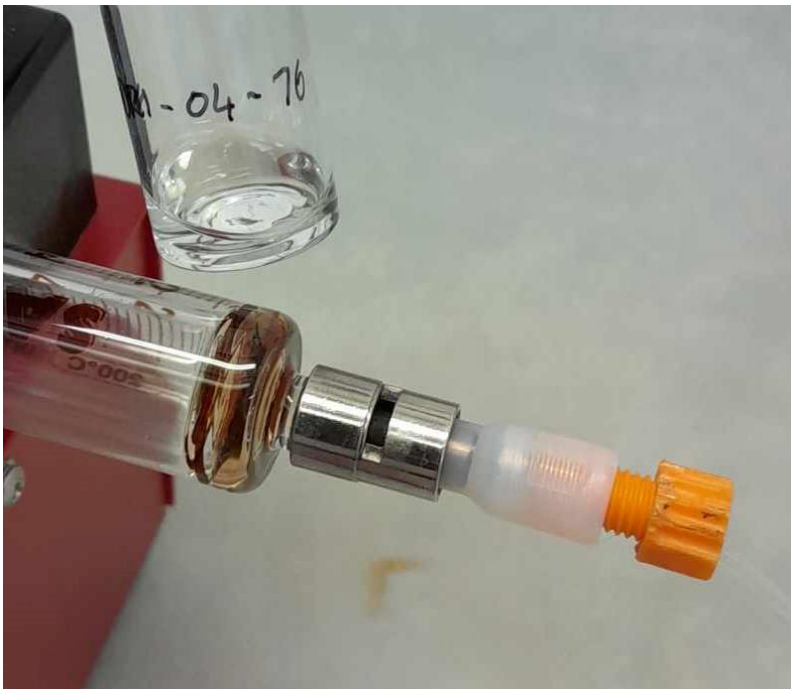

Figure S47: $NiCl_2$(dppp) solution in 1,4-dioxane/H_2O before (bottom) and after (top) electrolysis.

Lab book ref. DRH-04-76

9.6. Flow electrochemical recovery of Ni from NiCl(o-tolyl)(PPh_3)$_2$ catalysed SMCC

The reaction mixture following catalysis from Section 4.1 was analysed for Ni content prior to and following electrolysis. First, the solvent and other volatiles were removed *in vacuo*, then MeCN/H_2O (75:25 v/v, 5.2502 g) solvent was added to fully dissolve the residue, followed by PPh_4Br (142.8 mg). At this point, a sample was taken for NMR spectroscopy, mass spectrometry, LC and ICP analysis of reaction products and [Ni] determination. The rest of the mixture was processed using the electrochemical flow cell (flow rate = 0.075 mL min^{-1}, constant potential difference 2.0 V). A sample was collected at 3.000 mL to 3.950 mL (after 2 residence times) and analysed by NMR spectroscopy, mass spectrometry, LC and ICP analysis.

DRH-04-77-1 (stock solution of reaction mixture prior to electrolysis)

Concentration of Ni (LC method) = 0.66 mM

[Ligand] / mM = 0.267
[Ni]/[Ligand] ratio range = 0.02 – 0.07
(LCMS data lab book ref. DRH-04-78 C 14 to 19)

ICP 243.03 ppm, 4.14 mM (giving 18.2 mg of Ni complex in reaction. 17.8 mg of Ni complex was weighed into the reaction mixture, 4.05 mM)

Density of solvent = 0.848

DRH-04-77-2 (2 mL – 2.950 mL fraction after start of flow electrolysis. Reaction at steady state)

Concentration of Ni (LC method) = 0.67 mM
% Ni recovery (from 4.05 mM initial [Ni] = 83.5%
[Ligand] / mM = 0.267
[Ni]/[Ligand] ratio range = 0.04 – 0.08
(LCMS data lab book ref. DRH-04-78 D 20 to 25)

ICP 30.15 ppm, 0.51 mM

Density of solvent = 0.848

A change in [Ni] detected by ICP shows that Ni was indeed removed electrochemically from the sample. A likely reason for the underestimation by the LC method before electrochemical removal

is that the Ni species was present as polymers / higher order clusters. As such, only free Ni species could be ligated. Electrolysis will have broken down these Ni aggregates, allowing for the LC method to be deployed more efficiently. The organic product remained intact throughout the process (as evidenced by ^{1}H NMR spectroscopy and GC-MS (EI).

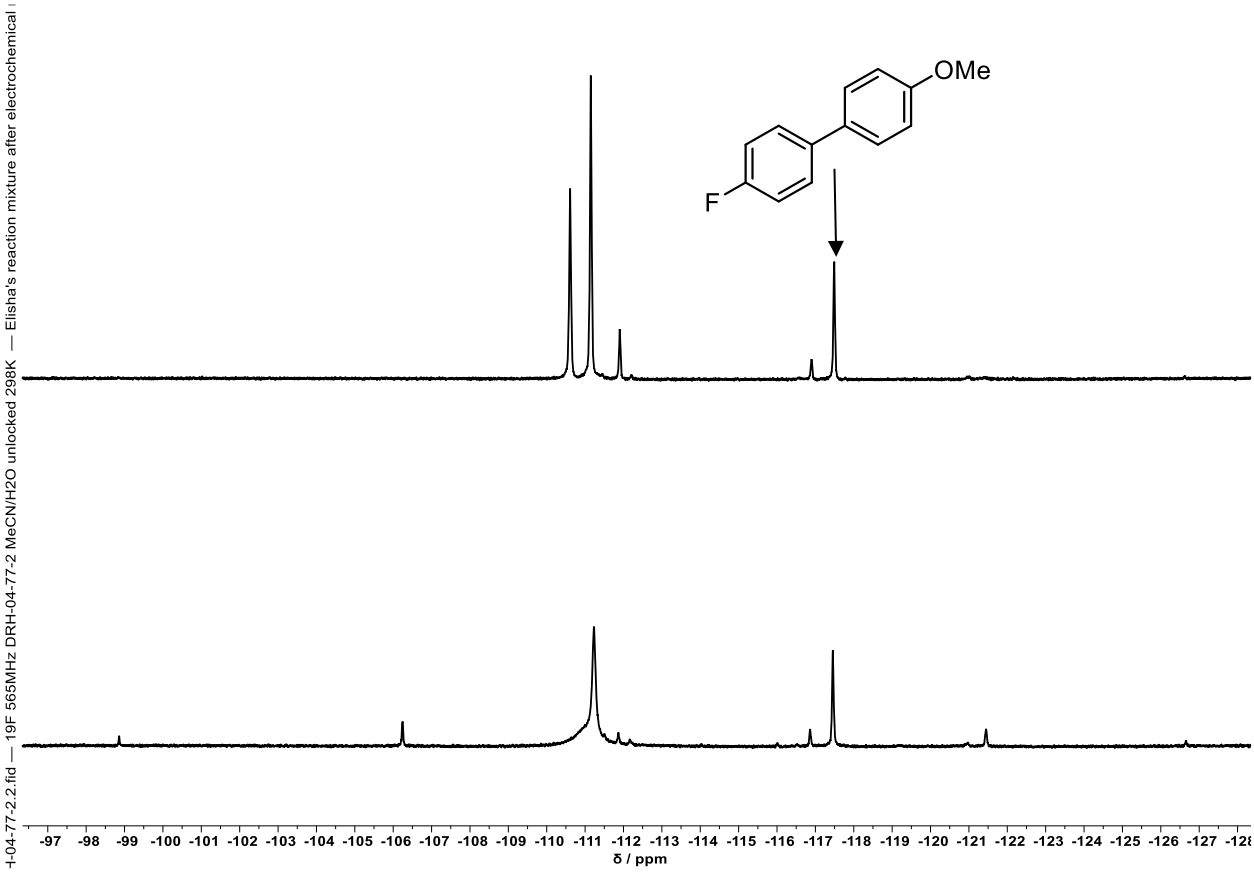

Figure S48: ^{19}F NMR spectra (565 MHz, MeCN/H_2O unlocked, 298 K) of reaction mixture prior to electrolysis (top), and reaction mixture after electrolysis (bottom). The product 6 peak (-117.5 ppm) remains unchanged, but the boronic acid peaks (-110 – 112 ppm region) are affected by the electrolysis.

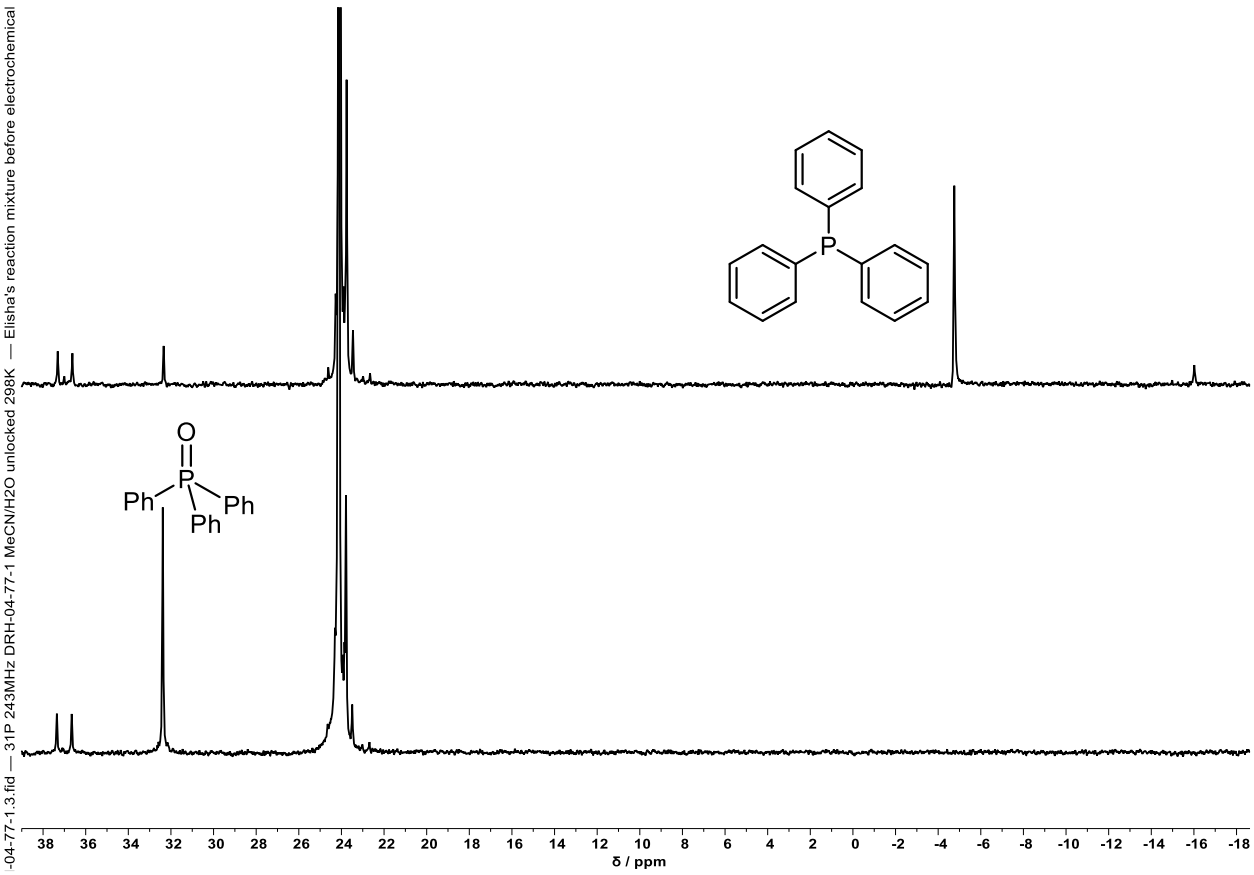

Figure S49: ^{31}P NMR spectra (243 MHz, MeCN/H_2O unlocked, 298 K) of reaction mixture prior to electrolysis (top), and reaction mixture after electrolysis (bottom). PPh_3 (-4.7 ppm) oxidises during electrolysis to the corresponding oxide (32.4 ppm), indicating that a redox process (i.e. with subsequent reduction of Ni^{2+}) has occurred.

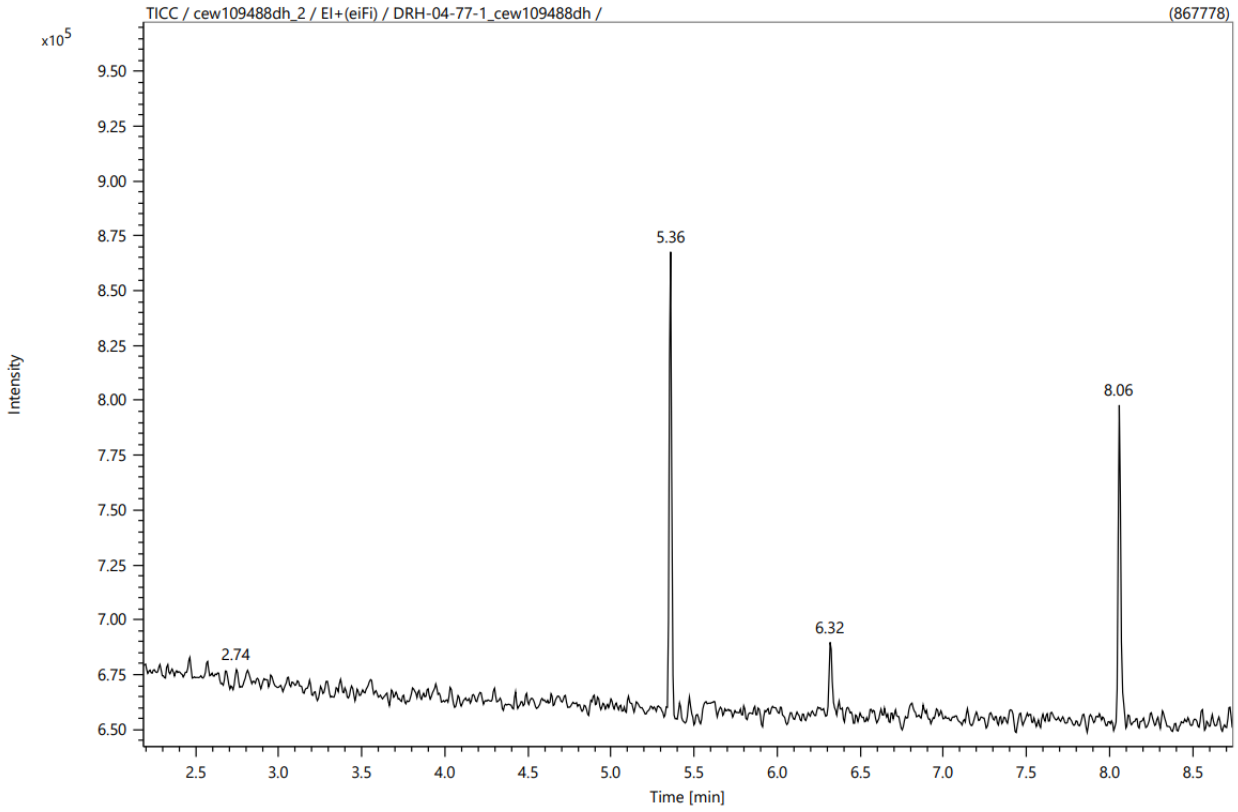

Figure S50: GC trace of the SMCC reaction mixture prior to electrolysis (lab book ref. DRH-04-77-1). The peak at 6.32 min was identified as organic product 6 (with comparison to authentic sample), and 8.06 min is PPh_3 (from a library mass hit).

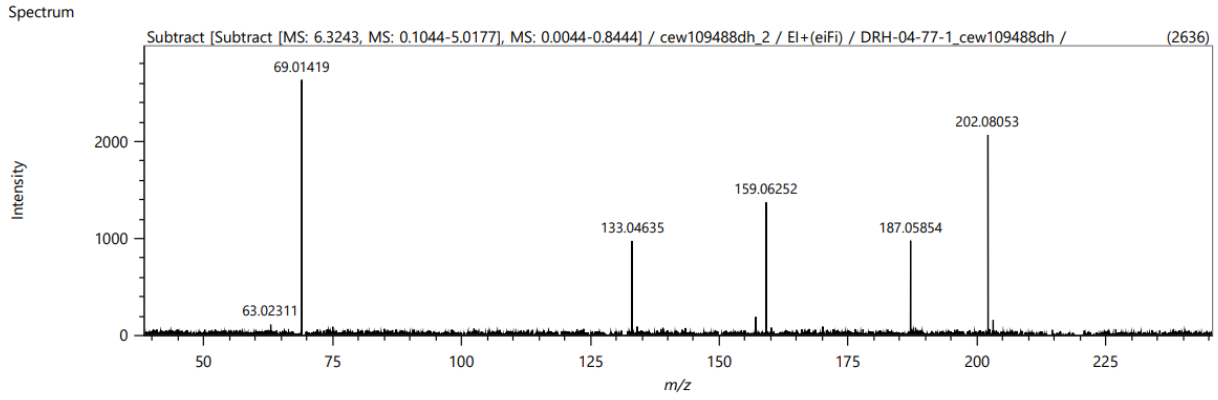

Elemental Composition

Parameters		Elements Set 3:				
Tolerance:	±40.00 ppm	Symbol	C	H	F	O
Electron:	Odd/Even	Min	6	4	1	1
Charge:	+1	Max	20	15	1	1
DBE:	-0.5 - 100.0					

Results

Mass	Intensity	Formula	Calculated Mass	Mass Difference [ppm]	DBE
202.08053	2067.54	C13 H11 O F	202.07884	8.33	8.0

FigureS51: HRMS (EI) spectrum of the GC peak at retention time 6.32 min confirming the presence of the SMCC product 6.

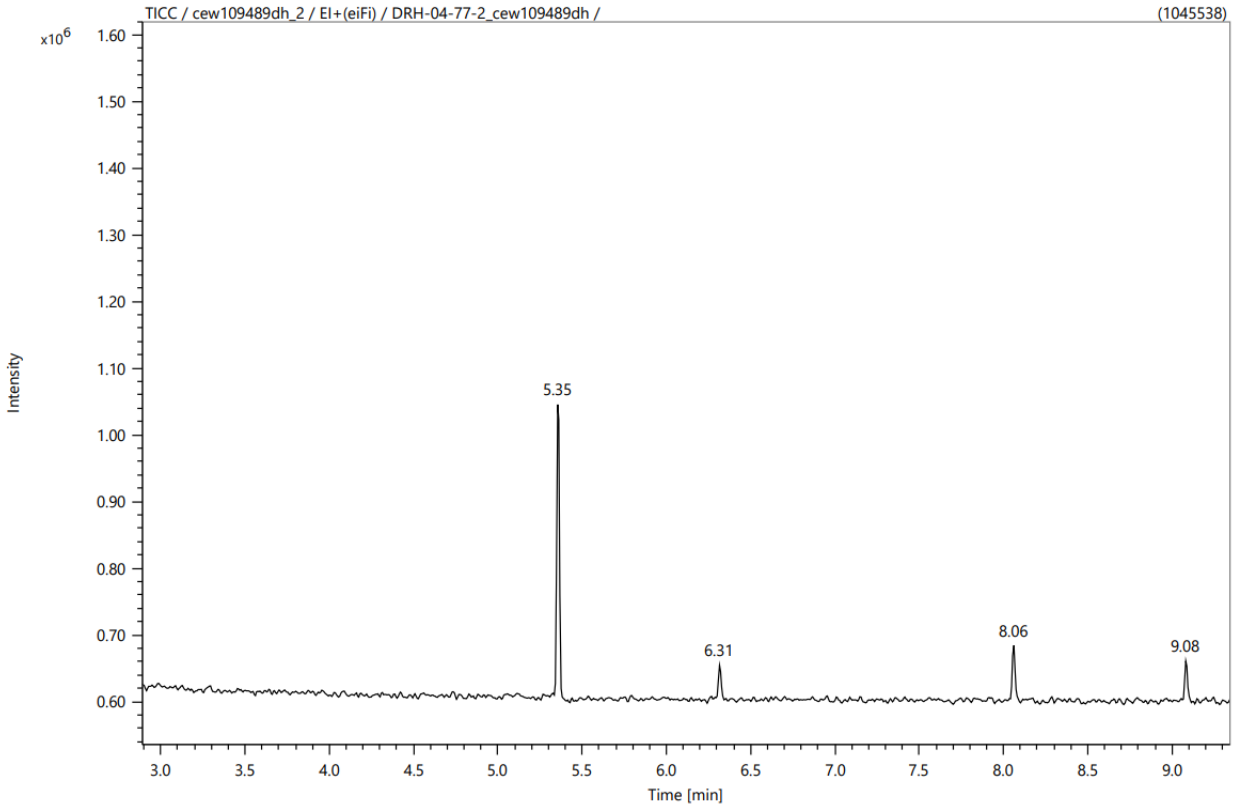

FigureS52: GC trace of the SMCC reaction mixture after electrolysis (lab book ref. DRH-04-77-2). The peak at 6.31 min was identified as product (with comparison to authentic sample), 8.06 min is PPh_3 (from a library mass hit), and 9.08 min is $O{=}PPh_3$ (from a library mass hit), confirming the generation of phosphine oxide during electrolysis. This also confirms that the SMCC product 6 remains intact during electrolysis.

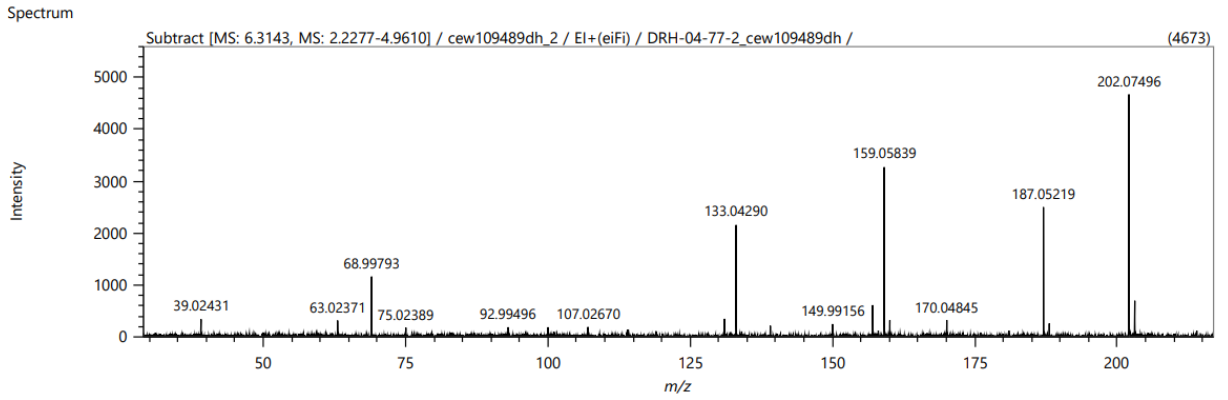

Elemental Composition

Parameters		Elements Set 3:				
Tolerance:	±40.00 ppm	Symbol	C	H	F	O
Electron:	Odd/Even	Min	6	4	1	1
Charge:	+1	Max	20	15	1	1
DBE:	-0.5 - 100.0					

Results

Mass	Intensity	Formula	Calculated Mass	Mass Difference [ppm]	DBE
202.07496	4672.53	C13 H11 O F	202.07884	-19.23	8.0

FigureS53: HRMS (EI) spectrum of the GC peak at retention time 6.31 min confirming the presence of the SMCC product 6.

Lab book ref. DRH-04-77

9.7. **Flow Electrochemical recovery of Ni from $NiCl_2$(dppp) catalysed SMCC**

The reaction mixture following catalysis from Section 4.2 was analysed for Ni content following electrolysis. An aliquot of the supernatant (3.2615 g) was mixed with deionised water (1.1171 g) and PPh_4Br (125 mg). 2 x SS (+ve, parallel), Graphite (-ve) electrodes, 2.3 V (constant voltage), 4 mA (initial current), flow rate = 0.075 mL min^{-1}, residence time = 12.37 min.

DRH-04-69-2 (2 mL – 2.7 mL fraction after start of flow electrolysis. Reaction at steady state)

Starting concentration Ni = 17.7 mM (theoretical)
End concentration Ni (LC method) = 4.78 mM
% Ni recovery = 73.0%
[Ligand] / mM = 0.319
[Ni]/[Ligand] ratio range = 0.25 – 0.42
(LCMS data lab book ref. DRH-04-70 G 37 to 42)

ICP 294.84 ppm, 5.02 mM

Density of solvent = 1.00

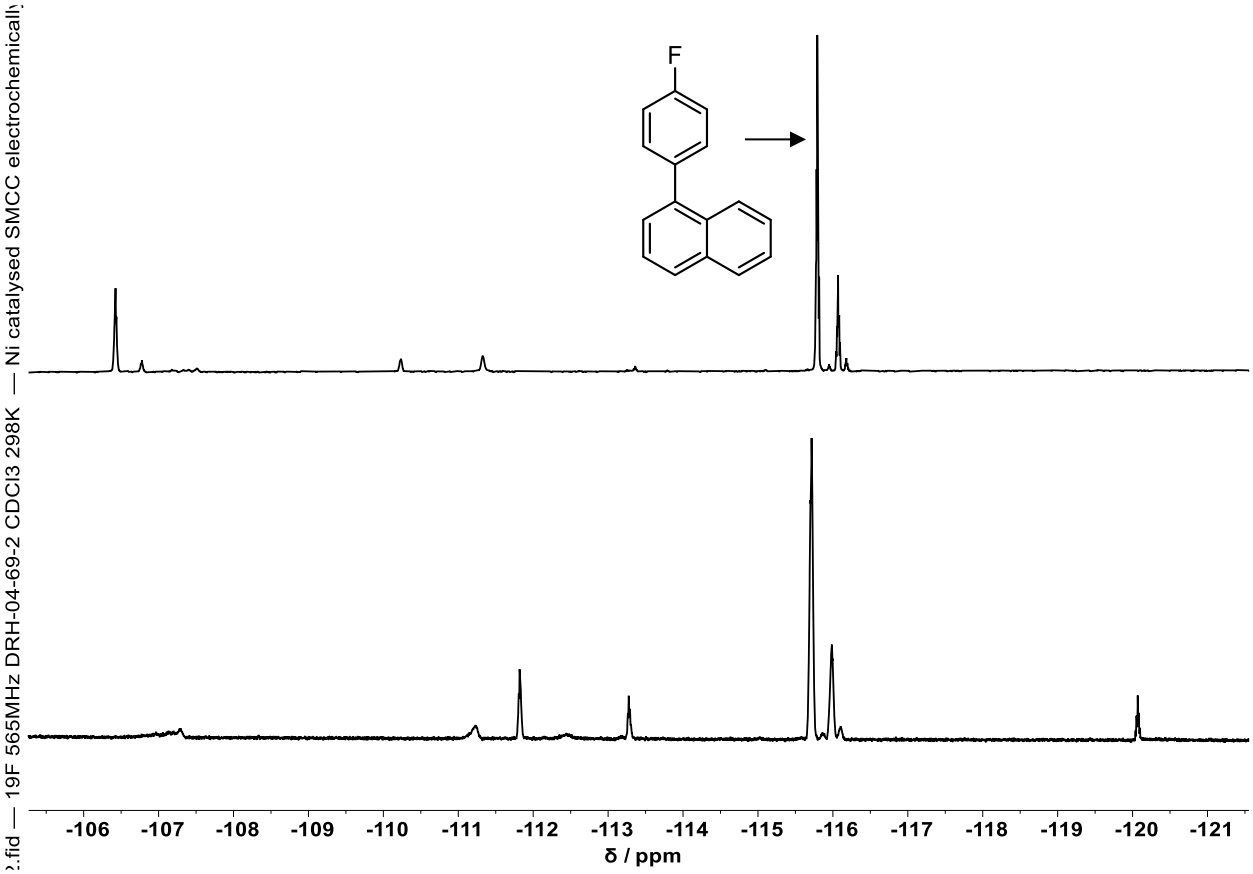

FigureS54: ^{19}F NMR spectra (565 MHz, C*D*Cl$_3$, 298 K) of the Ni-catalysed SMCC prior to electrolysis (top) (lab book ref. DRH-04-52) and after electrolysis (bottom) (lab book ref. DRH-04-69-2).

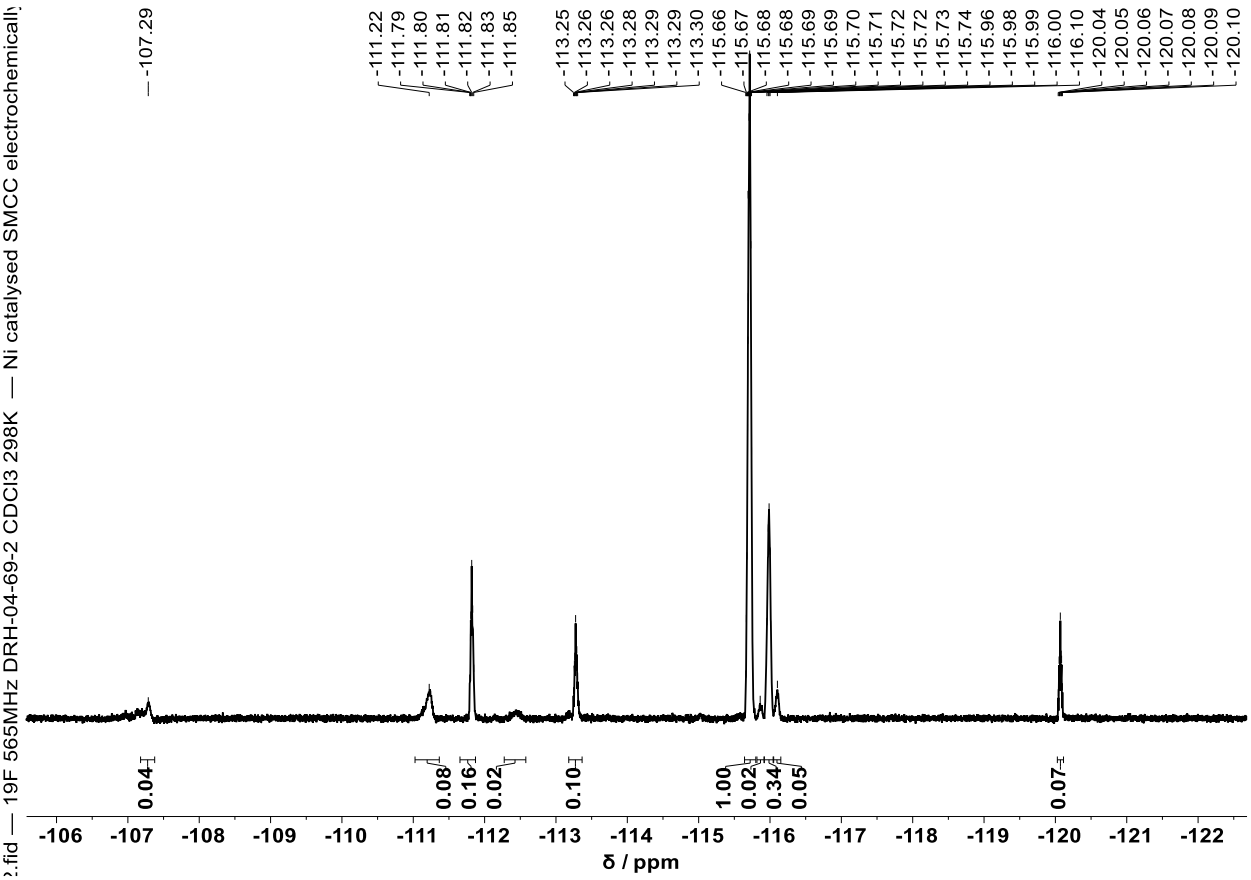

Figure 55: ^{19}F NMR (565 MHz, C*D*Cl$_3$, 298 K) of the SMCC reaction mixture after electrochemical recovery. Yield of product 7 = 88% (as a proportion of total ^{19}F environments after electrochemical recovery (c.f. 79% before)). This increase is likely due to a change in arylboronic acid speciation and peak broadening of the NMR spectra.

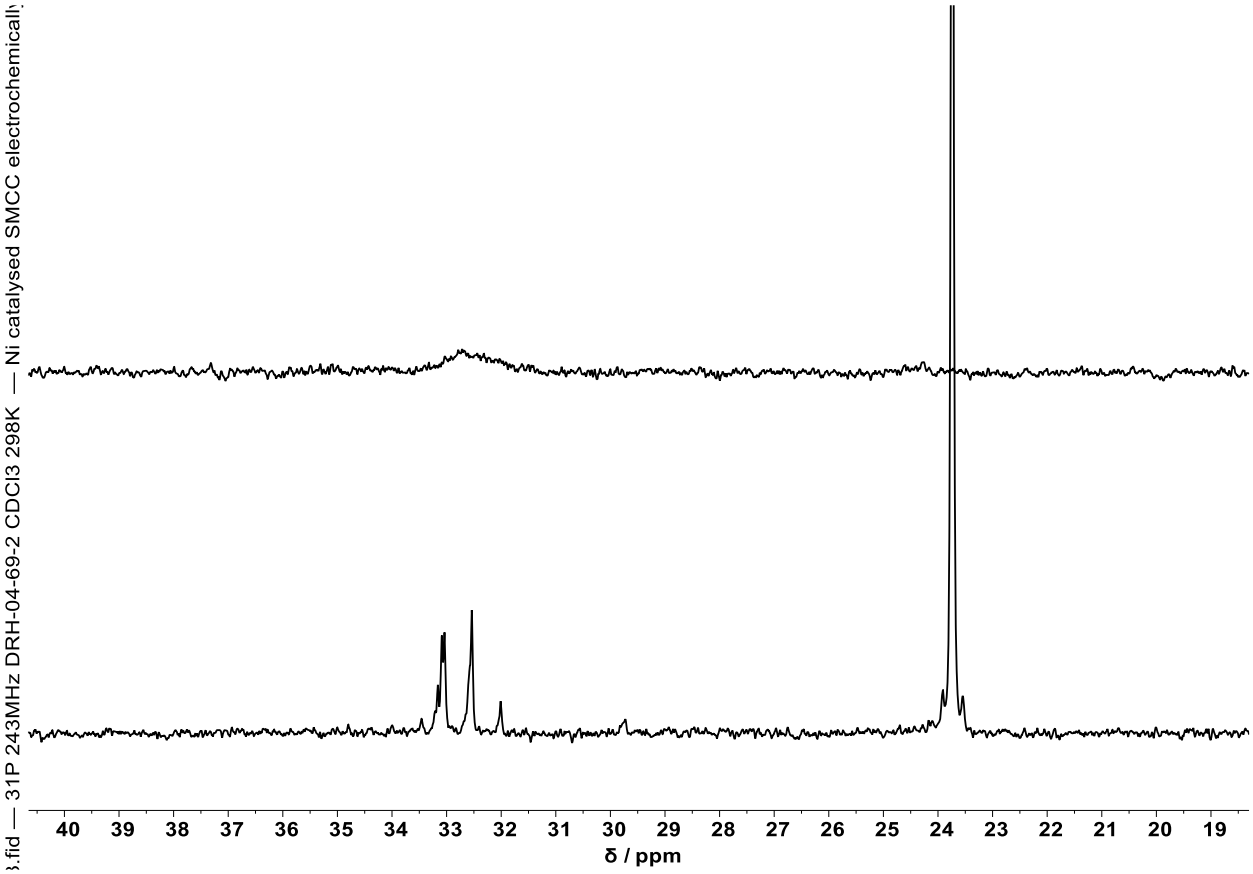

FigureS56: ^{31}P NMR spectra (243 MHz, C*D*Cl$_3$, 298 K) of the Ni-catalysed SMCC prior to electrolysis (top) (lab book ref. DRH-04-52) and after electrolysis (bottom) (with addition of PPh$_4$Br shown at 23.8 ppm (lab book ref. DRH-04-69-2). The lack of paramagnetic broadening in the ^{31}P NMR after electrolysis is an indication that no tetrahedral Ni is present.

Lab book ref. DRH-04-69

10. NMR spectra of synthesised compound

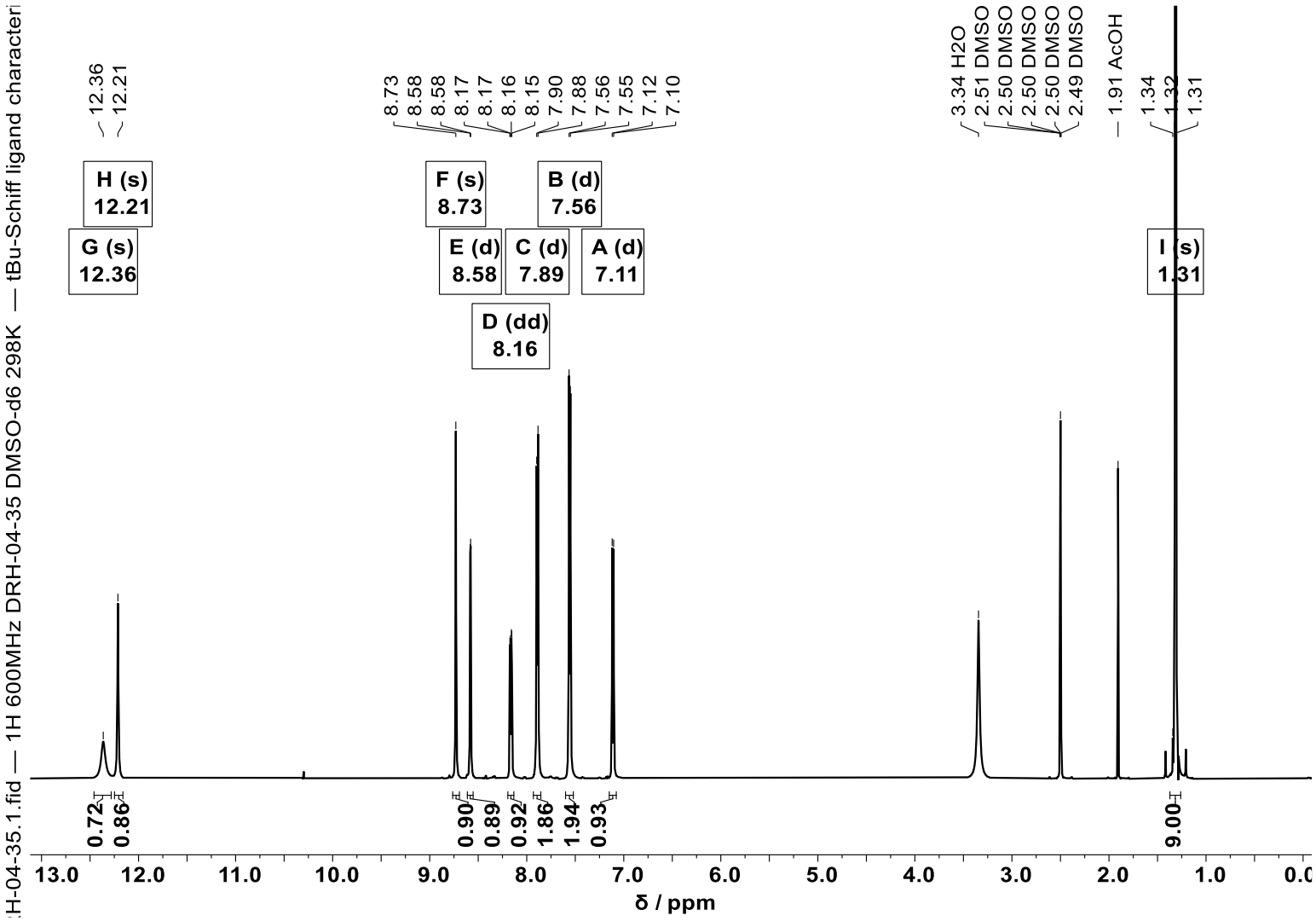

Figure S57: ^{1}H NMR spectrum (600 MHz, DMSO-d_6, 298 K) ^{t}Bu-Schiff ligand 1, lab book ref. DRH-04-35.

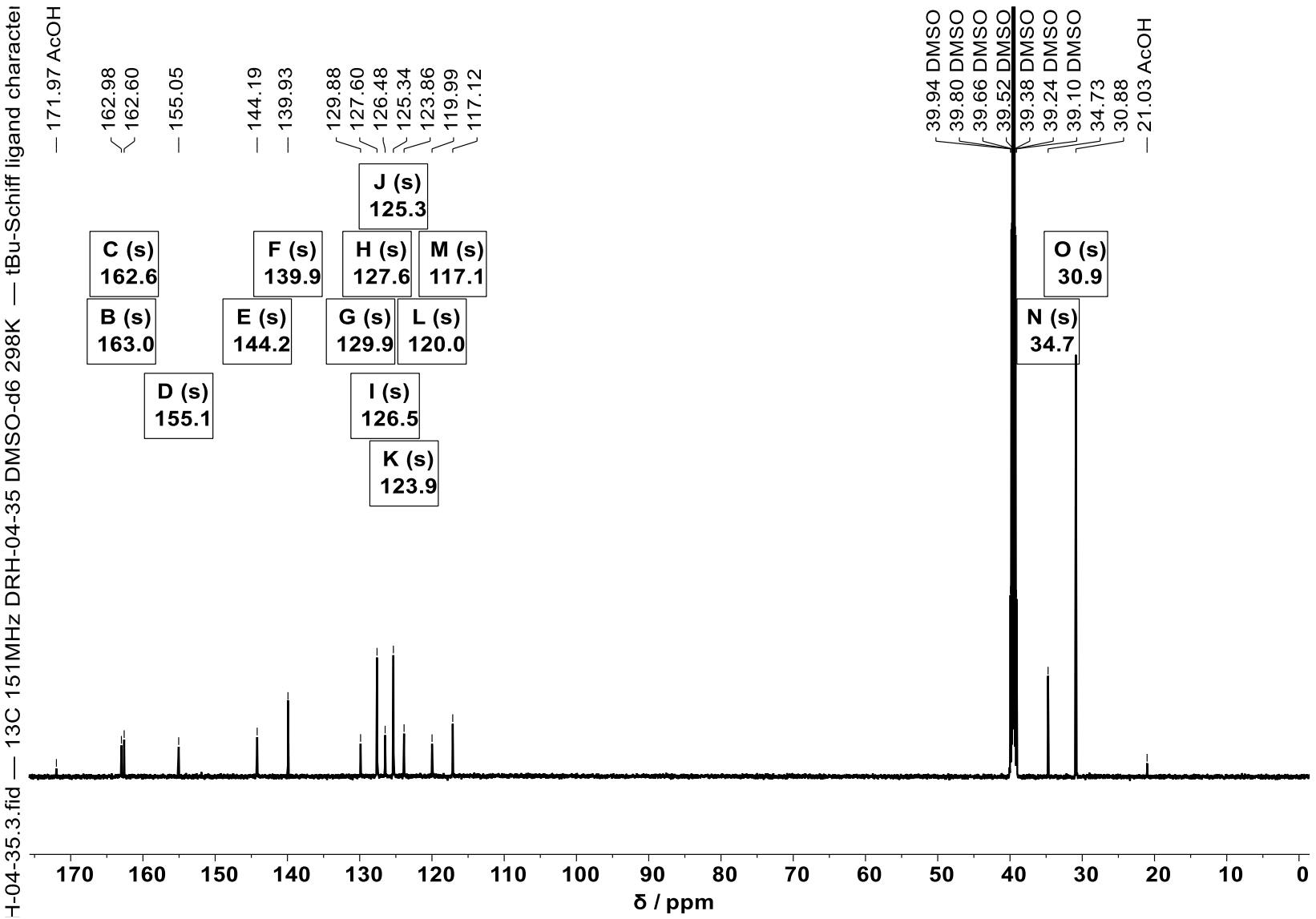

Figure S58: ^{13}C NMR spectrum (151 MHz, DMSO-d_6, 298 K) ^{t}Bu-Schiff ligand 1, lab book ref. DRH-04-35.

11. References

1 G. R. Fulmer, A. J. M. Miller, N. H. Sherden, H. E. Gottlieb, A. Nudelman, B. M. Stoltz, J. E. Bercaw and K. I. Goldberg, *Organometallics*, 2010, **29**, 2176–2179.

2 CrysAlisPro, Oxford Diffraction Ltd. Version 1.171.34.41.

3 Empirical absorption correction using spherical harmonics implemented in SCALE3 ABSPACK scaling algorithm within CrysAlisPro software, Oxford Diffraction Ltd. Version 1.171.34.40.

4 O. V. Dolomanov, L. J. Bourhis, R. J. Gildea, J. A. K. Howard and H. Puschmann, *J. Appl. Crystallogr.*, 2009, **42**, 339–341.

5 G. M. Sheldrick, *Acta Cryst. A*, 2015, **71**, 3–8.

6 J. Jacq, C. Einhorn and J. Einhorn, *Org. Lett.*, 2008, **10**, 3757–3760.

7 P. Melnyk, V. Leroux, C. Sergheraert and P. Grellier, *Bioorg. Med. Chem. Lett.*, 2006, **16**, 31–35.

8 X. Guo, H. Dang, S. R. Wisniewski and E. M. Simmons, *Organometallics*, 2022, **41**, 1269–1274.

9 Y.-L. Zhao, Y. Li, S.-M. Li, Y.-G. Zhou, F.-Y. Sun, L.-X. Gao and F.-S. Han, *Adv. Synth. Catal.*, 2011, **353**, 1543–1550.

10 C. Li, Y. Shi, Q. Chen, K. Zhang and G. Yang, *J. Org. Chem.*, 2023, **88**, 2306–2313.

11 K. Chen, W. Chen, X. Yi, W. Chen, M. Liu and H. Wu, *Chem. Commun.*, 2019, **55**, 9287–9290.

12 C. Schotten, J. Manson, T. W. Chamberlain, R. A. Bourne, B. N. Nguyen, N. Kapur and C. E. Willans, *Catal. Sci. Technol.*, 2022, **12**, 4266–4272.

13 T. P. Nicholls, R. A. Bourne, B. N. Nguyen, N. Kapur and Charlotte. E. Willans, *Inorg. Chem.*, 2021, **60**, 6976–6980.